Chapter 7

The Classification Indices-Based Model for NPP According to the Integrated Orderly Classification System of Grassland and Its Application

Huilong Lin

Additional information is available at the end of the chapter

http://dx.doi.org/10.5772/57297

1. Introduction

Grassland accounts for 25% of the world's land area and has global significance for climate-carbon feedback [1]. As one of the most widespread ecosystem types, grassland makes a large contribution to carbon sequestration and plays a significant role in regional climates and the global carbon cycle [2]. Grassland net primary productivity (NPP) refers to carbon accumulation (photosynthesis less respiration) in grassland per unit of time, and can be used as an indicator of the capacity of the grassland ecosystem to accumulate carbon and to support grazing animals. Studies of the NPP have contributed significantly to our understanding of the pattern, process and dynamics of grassland ecosystems. Hence, the accurate estimation of the NPP of grasslands is very important not only for scientifically guiding grassland management but also for understanding the global carbon cycle. Reliable long-term data on grassland NPP are urgently needed to estimate carbon fluxes. Due to their time- and labor-intensive nature, ground measurements of grassland NPP are very limited in temporal and spatial coverage. The precision evaluation of NPP estimated in regional or global scales is always very difficult. Direct measurement of grassland NPP is tedious and not practical for large areas, so it is therefore appropriate to use computer models, calibrated with existing data, to study the spatial and temporal variations of grassland NPP [3].

A number of different methods of modelling the dynamics of grassland NPP have been reported. In climate-vegetation models, empirical relationships are developed, allowing NPP to be estimated as a function of climate variables such as temperature, precipitation, and evaporation [4-12]. Process models for estimating NPP simulate a series of plant physiological processes and their response to changes in environmental factors, including photosynthesis,

autotrophic respiration and transpiration [13, 14]. In spite of this, the body of knowledge of basic biological mechanisms to simulate grassland NPP is still limited. Furthermore, process models cannot be used in developing countries because long-term data required for the parameters of the models is not available. Algorithms for estimating NPP by remote sensing may be poorly parameterized if the 'calibration' estimates of NPP are based upon an inappropriate method. In this respect, climate-vegetation models have been drawing much attention and have been widely applied internationally, owing to their simplicity [4]. These models have been shown to yield 'reasonable estimates' of regional or global NPP distribution [4, 9, 14-16].

Vegetative types and their distribution pattern can be related to certain climatic types in a series of mathematical forms. Thus, the climate can be used to predict vegetative types and their distribution, or the reverse [17]. A growing number of research efforts have demonstrated the importance of climate-vegetation interaction in understanding climate sensitivity and climate change [18]. However, current climate-vegetation classification models mostly simulate the equilibrium state of vegetation types, and do not include NPP [19]. Furthermore, at present there is no vegetation-climate model based on a classification system including the NPP function. Therefore, development of climate-vegetation classification models coupled with NPP is urgently needed in order to evaluate the possible impacts of global change on terrestrial vegetation types [19]. So the focus of future research should be to master the link between NPP and grassland class, and to develop pertinent NPP models under a consistent classification system.

2. The classification indices-based model according to the Integrated Orderly Classification System of Grassland (IOCSG)

A grassland classification system, named the Integrated Orderly Classification System of Grassland (IOCSG), uses the factors Growing Degree Days (GDD), MAP (mean annual precipitation) and the moisture index (K value) to classify grassland diversity [17]. The theory behind the IOCSG has been developed in the last 60 years since it was first put forward in the 1950s, and it has achieved widespread use in China [17, 20]. Liang et al. [20] compared the change in potential vegetation distributions from 1911 to 2000 between the IOCSG, the Holdridge Life Zone [5] and BIOME4 [21]. Their results show that the IOCSG has the advantage of being simple and operational in its simulation of grassland classes, making it by far the best grassland classification system.

The Classification Indices-based Model, dubbed the Holdridge life-zone system [5], and the IOCSG [17] were originally built using eco-physiological features and a regional evapotranspiration model with the elimination of the common variable RDI (radioactive dryness index) by the chain rule. It results in a value for NPP (Mg DM ha^{-1} yr^{-1}) as a function of GDD and the moisture index (K value). Its ecological base is the IOCSG [17, 20, 22-25]. The method of integrating the classification indices of IOCSG to estimate the NPP is of the form:

http://dx.doi.org/10.5772/57297

$$NPP = \frac{0.1GDD \cdot L^{2}(K) \cdot e^{-\sqrt{13.55+3.17K^{-1}-0.16K^{-2}+0.0032K^{-3}}} \cdot (K^{6} + L(K)K^{3} + L^{2}(K))}{[(K^{6} + L^{2}(K)) \cdot (K^{5} + L(K)K^{2})]}$$

Where GDD is defined as the mean of positive unit-period temperatures with the substitution of zero for all unit-period values below 0 °C. The K value is the ratio of MAP to GDD, which provides an index of biological humidity conditions.

$$K = MAP / 0.1GDD,\ L(K) = 0.58802K^{3} + 0.50698K^{2} - 0.0257081K + 0.0005163874$$

The Classification Indices-based Model not only has the advantage of being simple, operational, and especially compatible with the IOCSG used to derive NPP from its class, it also responds to dynamic vegetation-climate relationships.

3. Model validation and model inter-comparison

Model inter-comparison has been used as an alternative method for indirect validation and identification of model weaknesses and inconsistencies where ground observations are lacking [26]. However, a simultaneous comparison of these climate-vegetation models to estimate grassland NPP, using a consistent classification system, has not been attempted on a regional, China-wide or global scale.

The following three performance indicators were used as the model evaluation and performance criteria: (1) the mean bias error (MBE) [24,27,28]; (2) the coefficient of variation of the root-mean-square error (CVRMSE), which is defined as the RMSE normalized to the mean of the observed values; and (3) the forecast efficiency, E [29]. The prediction is considered excellent with the CVRMSE < 10%, good if 10-20%, fair if 20-30%, poor if >30% [30]. CVRMSE is the relative difference between the simulated and observed data, while the Nash-Sutcliffe model efficiency statistic (E) [29], regarded as a measure of the overall fit between observed and predicted values, is the primary criterion.

For the purpose of comparison with model simulations, the observed or predicted NPP was expressed in g C m^{-2} per year, where 1 g carbon is equivalent to 2.2 g oven-dried organic matter [31-34].

3.1. Evaluation of seven methods to predict grassland net primary productivity along an altitudinal gradient in the Alxa Rangeland, Western Inner Mongolia, China

China's grasslands are mainly distributed in arid and semi-arid areas of West China [35]. The main grassland classes within China are Temperate meadow-steppe, Steppe and Desert-steppe [35, 36]. Helan Mountain (elevation 3556 m), located in an ecologically vulnerable area of the northwestern part of China, further enriches the diversity of vertical grassland classes. The rangeland classes change from the high to low elevation: Alpine meadow, Steppe, Desert steppe, Steppe desert, and Desert. Thus, Helan Mountain provides an ideal target system to validate the Classification Indices-based Model and test IOCSG theory, which can be done

from plots to estimate landscape-scale effects, something that so far has proven to be a challenge to ecologists worldwide [37].

This study continues our efforts to develop a robust estimation capability of NPP for grassland and, specifically, verifies the grassland NPP estimates from the climate-vegetation models along an altitudinal gradient on Helan Mountain and in the surrounding desert rangeland. The specific research objectives are to: 1) compare field-measured NPP based on field-observed data among different grassland classes along an altitudinal gradient in the Helan Mountain range and the surrounding desert; 2) compare and evaluate NPP estimated from the Miami Model [6], Thornthwaite Memorial Model [38], Schuur Model [15], Chikugo Model [8], Beijing Model [12], Synthetic Model [10,11,39], and the Classification Indices-based Model [22,24,25,27,28] with NPP derived from measurements at eight sites in the region; and 3) evaluate the applicability and reliability of the seven models among these grassland classes.

3.1.1. Study area and methods

3.1.1.1. Study area and site descriptions

The study area is located along the northern slopes of the Helan Mountain and the surrounding Alxa Desert (long. 105°32′ to 105°51′, lat. 38°39′ to 39°19′; alt. 3556 m to1360 m a.s.l.), in western Inner Mongolia (Figure 1). Eight study sites were selected following annual rainfall gradient variations with respect to grassland classes at three altitudes that represent the full range of grassland vegetation, environmental, terrain and soil conditions (Figure 1). Based on the historical meteorological data among the eight study sites, GDD and the moisture index (K value) were calculated. According to the IOCSG, the grasslands at the eight sites were classified into five classes: Alpine meadow (site 1), Cold temperate-humid montane meadow (site 2), Cool temperate-sub-humid meadow steppe (site 3), Cool temperate-semiarid temperate typical steppe (site 4) and Cool temperate-arid temperate zonal semi-desert (sites 5-8), respectively (Figure 1).

3.1.1.2. Plots-based NPP collection

The total observed NPP dataset was the sum of above- and below-ground NPP, following standard methods [3,40,41], and it was based on averages of five duplicated plots at each sampling site from April to October once every month for three consecutive years (2003-2005). One hundred and twenty plot-based NPP sets from the eight study sites were obtained [25].

3.1.2. Results

3.1.2.1. Descriptive statistics of observed NPP

The gradient distribution of grassland classes varied in different NPP values among the study sites. With all data pooled together, the observed NPP values of the Cool temperate-arid temperate zonal semi-desert has an extreme degree of variation, ranging from 72.60 to 242.02 g C m^{-2} per year, with a coefficient of variation of 28.38%. The mean NPP of the

http://dx.doi.org/10.5772/57297

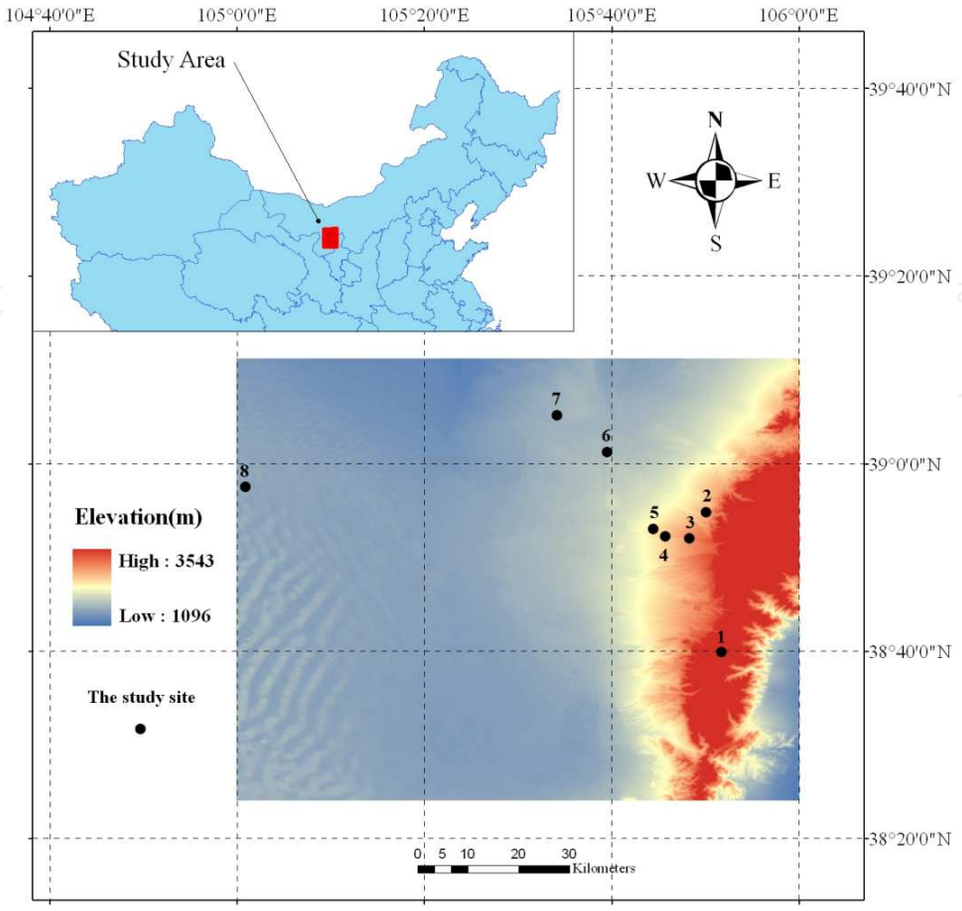

Figure 1. Location map of study area and study sites. Dark circles represent the study sites in elevation. Arabic numerals denote the study site

Cool temperate-arid temperate zonal semi-desert was the lowest (133.43 g C m^{-2} per year), followed by that of Cool temperate-semiarid temperate typical steppe (160.57 g C m^{-2} per year), Cool temperate-subhumid meadow steppe (171.94 g C m^{-2} per year) and Alpine meadow (185.88 g C m^{-2} per year). The mean NPP of Cold temperate-humid montane meadow was the largest (192.54 g C m^{-2} per year).

3.1.2.2. Comparison of the seven models in terms model performance values

The performance of each of the seven models compared and evaluated in this study is also shown graphically by plotting predicted NPP values as a function of measured values, as presented in Figure 2. The biases that each model introduces are reflected at the relative positions of the 1:1 line. Data points above the 1:1 line are over-predicted while those under the 1:1 line are under-predicted. It can be seen that the Thornthwaite Memorial Model, Beijing Model and Miami Model over-predicted grassland NPP while the Synthetic Model and Schuur Model slightly under-predicted those quantities. Considering the slopes and intercepts for the regression of predicted NPP by the Chikugo Model and Classification Indices-based Model versus observed NPP, the regression of the Chikugo Model has a slope (0.9878) approximately equal to that (0.9873) of the Classification Indices-based Model, but the intercept (11.13) of the

regression line of the Classification Indices-based Model is much closer to zero than that (17.13) of the regression line of the Chikugo Model.

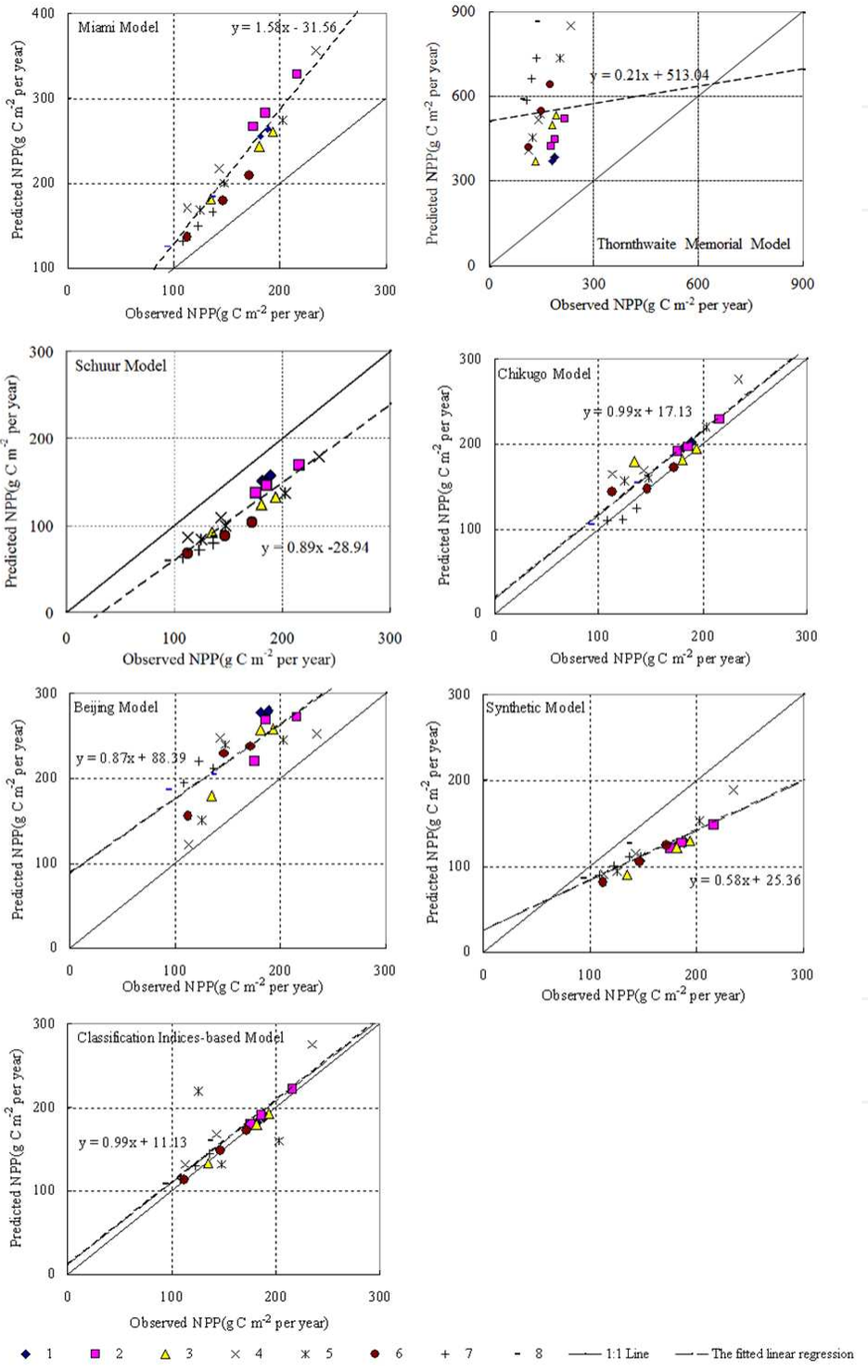

Figure 2. Predicted net primary productivity (NPP) versus Observed NPP from seven different models compared in this study. Each data point represents average of five replicates. Arabic numeral denotes the study site No..

http://dx.doi.org/10.5772/57297

Accordingly, the high values of E (0.67 and 0.87) in predicting NPP using the Chikugo Model and the Classification Indices-based Model indicate that these models outperform the others. The fitted linear regressions (intercepts are forced to zero) between the observed NPP and the methods are: the predicted NPP by Chikugo Model=1.09×Observed NPP, the predicted NPP by Classification Indices-based Model=1.05×Observed NPP, respectively. The results indicate that predicted NPP by the Classification Indices-based Model has a closer correlation with the observed NPP compared to the predicted NPP by the Chikugo Model. With E value of -0.27, -0.45, -1.79 and -2.61 for predicting NPP, respectively, the Synthetic Model, Schuur Model, Miami Model and Beijing Model ranked third, fourth, fifth and sixth. With E value of-113.16, the Thornthwaite Memorial Model was the least suitable. Overall, comparison of the predicted with the observed grassland NPP indicated that the CVRMSE value using the Classification Indices-based Model was less than 10%, which denotes that the prediction suitability of the Classification Indices-based Model is considered excellent, while the prediction of the Chikugo Model is considered good with CVRMSE=14.29%. As the CVRMSE value using the Synthetic Model is 28.19%, the prediction of the model is considered fair. Because of the CVRMSE values beyond 30%, the prediction using the other models is considered poor (Table 1).

Model	CVRMSE(%)	E	Ranked
Miami Model	41.84	-1.79	5
Thornthwaite Memorial Model	267.59	-113.16	7
Schuur Model	30.14	-0.45	4
Chikugo Model	14.29	0.67	2
Beijing Model	47.57	-2.61	6
Synthetic Model	28.19	-0.27	3
Classification Indices-based Model	8.98	0.87	1

Table 1. Comparison of the seven models in terms model performance values

3.1.3. Discussion

Seven different methods were compared in terms of their performance in predicting grassland NPP. The relatively high model efficiency in predicting grassland NPP using the Classification Indices-based Model and Chikugo Model indicates that these models outperform the others. The comparison of models involves the input data requirements from each model into account, as these factors affect the value of model efficiency (E), if they are optimized to maximize E. Generally, models with a large number of input variables and parameters would result in higher values of E than models with a small number of input variables and parameters. When comparing the Chikugo Model with the Classification Indices-based Model, it is evident that the Chikugo Model is more complicated in structure and highly intensive in its data requirements. The Chikugo Model provides insight into the relative importance of individual environmental variables in the evapotranspira-

tion process [7, 11, 42, 43]. The model is a mechanistic approach to estimate grassland NPP and always slightly overestimated the actual NPP. Furthermore, the Classification Indices-based Model is based on the IOCSG and used the classification indices as independent variables. It not only takes into account dynamic grassland classes [17], but also simulates NPP of corresponding grassland classes [22, 24, 25, 27, 28]. Thus it can be very easy to implement and understand. These factors support the Classification Indices-based model as a more accurate prediction among grassland classes in this study. So the Classification Indices-based Model was found to be the best choice for the given grassland classes. The model is especially suitable for grassland NPP research and application in many developing/undeveloped countries or regions that generally lack the detailed and complex observation data required by other models (i.e., BIOME4).

The results presented in this study were not only specific to this region, but more importantly, were specific to the given grassland classes according to the IOCSG approach, which can be scaled up from plots to estimate landscape-scale effects. The ascending order of grassland NPP and its class may have significant implications for grassland succession in Chinese grassland ecosystems with predicted changes in spatio-temporal patterns of precipitation under the influence of global climate change. So there is a need to extrapolate in order to calculate the grassland's response to climate change (for instance changing temperature and rainfall). Continued climate change is expected to result in changes in temperature and precipitation, the same as the changes along the altitudinal gradient in this study area. The changing climate will in turn affect the growth of plants, and result in changes to grassland classes and subsequently NPP. The combined affect of precipitation and temperature, that is, the moisture index (K), is to some extent most important to NPP spatial distribution. Thus, the Classification Indices-based Model has the potential to evaluate the possible effects of climate change on grassland classes and their NPP in the future, in order to improve the accuracy of NPP prediction and reduce the evaluation uncertainty of the possible effects of climate change in the future.

3.2. Model validation and modelling the potential net primary productivity of grassland in China

China is located in the southeast monsoon climate of the Eurasian continent, and covers a vast territory, with complicated terrain and distinctive distribution patterns of temperature and precipitation with different climatic zones, ranging from cold temperate to tropical and from moist to extreme drought. In addition, the ascent of the Qinghai-Tibetan Plateau(the so-called third polar region of the world) leads to a special plateau climate and thus forms a special pattern of vegetation distribution, termed as 'plateau zonality of vegetation' to distinguish horizontal zonality and vertical zonality of vegetation. The vegetation distribution of China can be characterized by the latitudinal zonality, longitudinal zonality, vertical zonality, and plateau zonality [44]. Thus, China's climate is unique and forms a special pattern of vegetation distribution. Grasslands account for 41.7% of land area in China [17]. Traditionally, China's grasslands have been economically productive areas and have provided important natural resources for the nation, including meat, milk,

http://dx.doi.org/10.5772/57297

wool and animal hides [35]. Grassland NPP can be used as an indicator of the capacity of the grassland ecosystem to accumulate carbon and to support grazing animals. The ability to accurately estimate grassland NPP is critical to our understanding of grassland dynamics [45]. But evaluation of the precision of grassland NPP estimates in China is difficult. Since it is a developing country, some mechanistic models cannot be used because long-term data required for the parameters of these models are not available in China [16]. But the required data are available for NPP-climate models, and these models have been shown to yield 'reasonable estimates' of global patterns of productivity [4, 9, 14, 16]. A growing number of research efforts [18] are focused on developing NPP-climate relationships. The Miami Model [38], the Schuur Model [15] and the Classification Indices-based Model [22, 24, 25, 27, 28] are examples of such efforts. But a simultaneous comparison using a consistent classification system has not been attempted in China.

The purpose of this section is: 1) to compared NPP estimated using the Miami Model [38], Schuur Model [15], and the Classification Indices-based Model [22,24,25,27,28] with NPP derived from measurements at 3767 sites in China, to evaluate the applicability and reliability of the Classification Indices-based Model; and 2) to simulate the spatial distribution patterns and its NPP characteristics of China's potential grassland under current climate scenarios using the IOCSG approach and NPP-climate models.

3.2.1. Data acquisition and methods

3.2.1.1. Observed NPP database

A large reference data set (n = 3767) of observations of grassland NPP with paired climatic variables was compiled for this study. This data set came from surveys conducted by the National Animal Husbandry and Veterinary Service of the Ministry of Agriculture of the People's Republic of China from 2004 to 2005. Total observed NPP dataset from the 3767 sites was the sum of above- and belowground NPP following the standard methods [3, 40] and it was based on the average of five duplicated plots at each sampling site. Locations of 3767 sampling sites were plotted using their associated geographic coordinates, as shown in Figure 3.

3.2.1.2. Climate data

Meteorological data for annual rainfall and GDD at 2348 meteorological stations, including longitude, latitude and altitude data of each meteorological station, were obtained from a database of the China Meteorological Data Sharing Service System from 1961 to 1990 (downloaded from the website: http://cdc.cma.gov.cn). The locations of the 2348 meteorological stations are shown in Figure 4. The Digital Elevation Model (DEM) was derived from the global 1km×1km DEM issued by the U.S. Geological Survey (USGS) (downloaded from the website: http://edcdaac.usgs.gov/gtopo30/ README. asp#h17). Regional data were derived from a database of 1:4 million Chinese regional data points, which was last updated in May 2004, and were used to confirm the Chinese boundary.

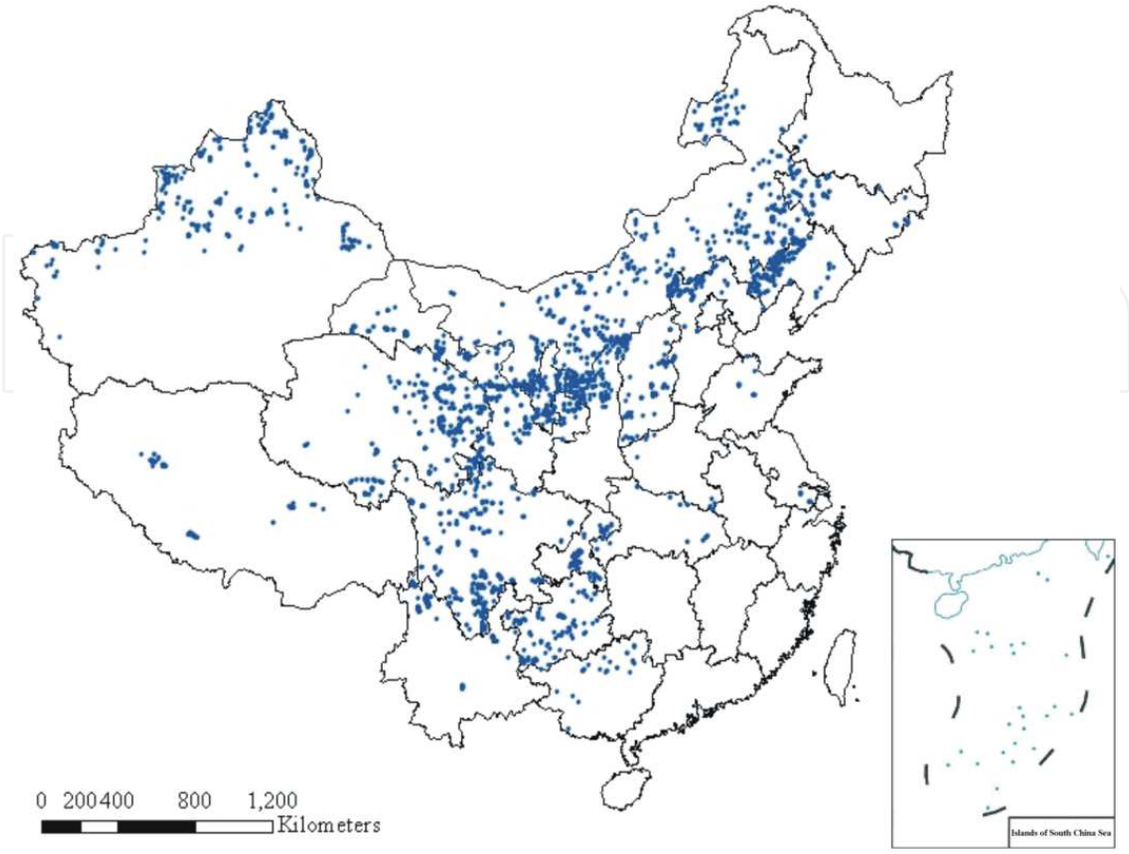

Figure 3. Locations of observation sites of grassland NPP in China.

3.2.1.3. Estimating grassland NPP and its distribution patterns in China

Spatialization of GDD and K value was created by introduction into the interpolation analysis of meteorological elements. The 1km×1km grid data of the moisture index averaged over years was obtained by the Kriging interpolation method (Figure 5). The inverse distance squared method (IDS) [46], modified by DEM in the smaller regions, was used to spatialize GDD data and to improve the interpolation precision of GDD in China [47]. By mosaicking the grid data of GDD on the actual ground of eight smaller areas and clipping the integrated interpolation area by the Chinese regionalism, we finally obtained the 1km×1km grid data of GDD (Figure 6). The 1km×1km grid data of the moisture index and GDD were used to predict the potential classes recognized by the IOCSG (Figure 7), and were then used to drive the Miami Model, Schuur Model, and the Classification Indices-based Model, respectively. To more explicitly reflect the spatial distribution patterns of potential biomes in China, and for ease of comparison and application, we merged the 42 classes of IOCSG to Grassland and Forest categories. The Grassland category consists of seven grassland super-class groups (biomes): Tundra and alpine steppe, Frigid desert, Semi-desert, Steppe, Temperate humid grassland, Warm desert and Savanna. The Forest category includes Temperate forest, Sub-tropical forest and Tropical forest (Table 2). The summed NPP has a unit of g C for pixels or Tg C (1 Tg = 10^{12}g) for each grassland super-class group (biome) or Pg C (1 Pg = 10^{15}g) for Grassland or Forest category in China.

http://dx.doi.org/10.5772/57297

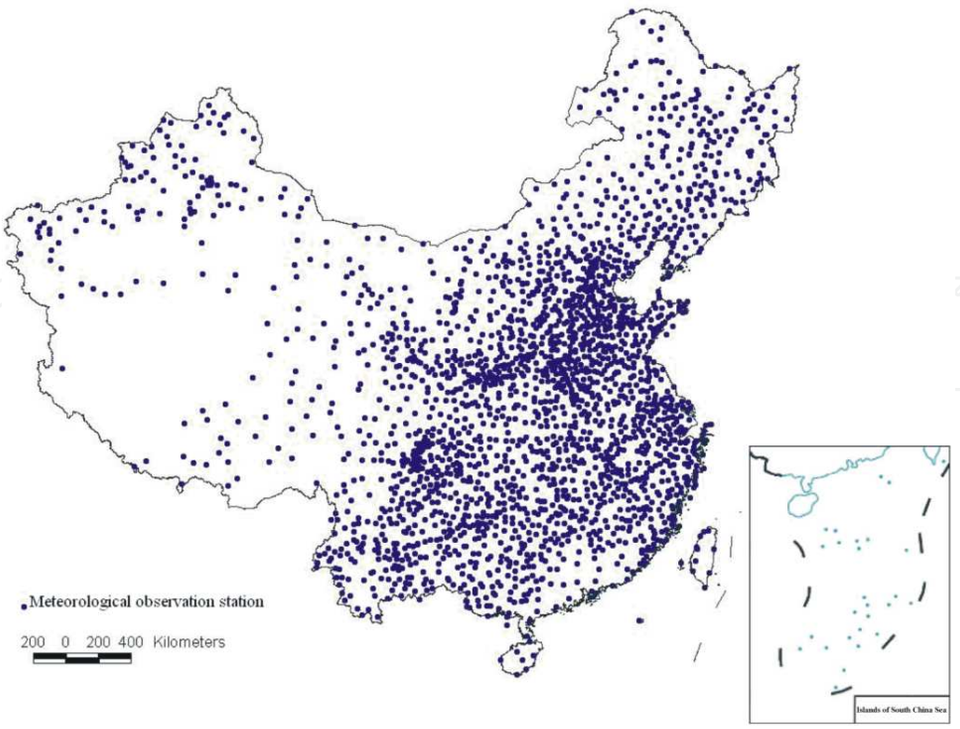

Figure 4. Spatial distribution of 2348 meteorological observation stations used for plotting spatial distribution of GDD and K value

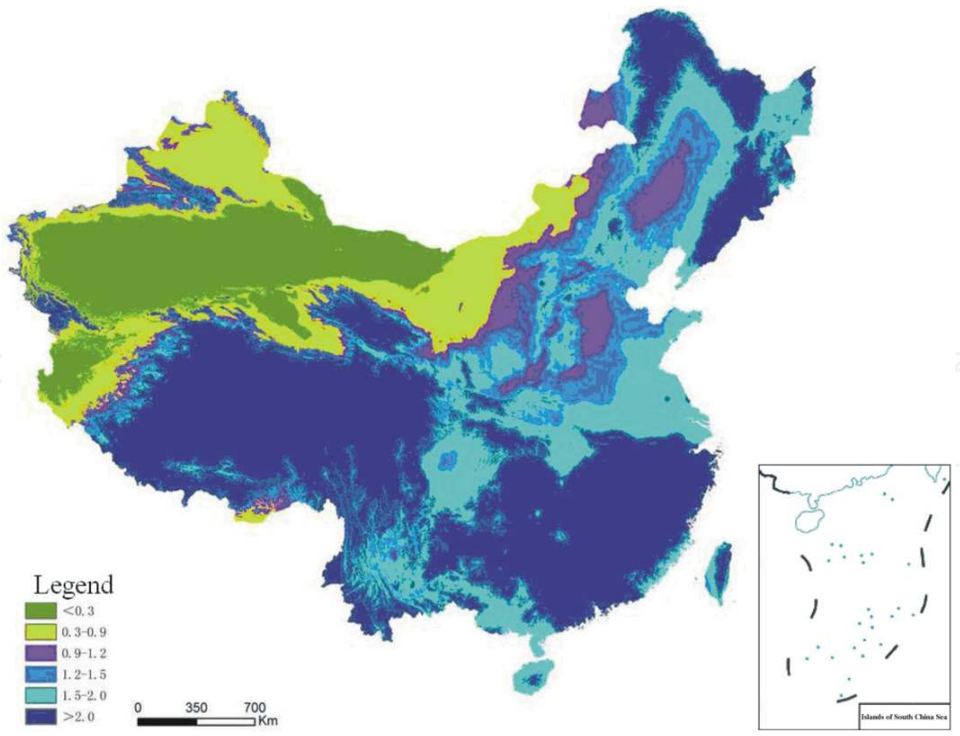

Figure 5. 1km x 1km grid map of China showing the moisture index (K value) obtained by Kriging interpolation. The legends show the zones of K value.

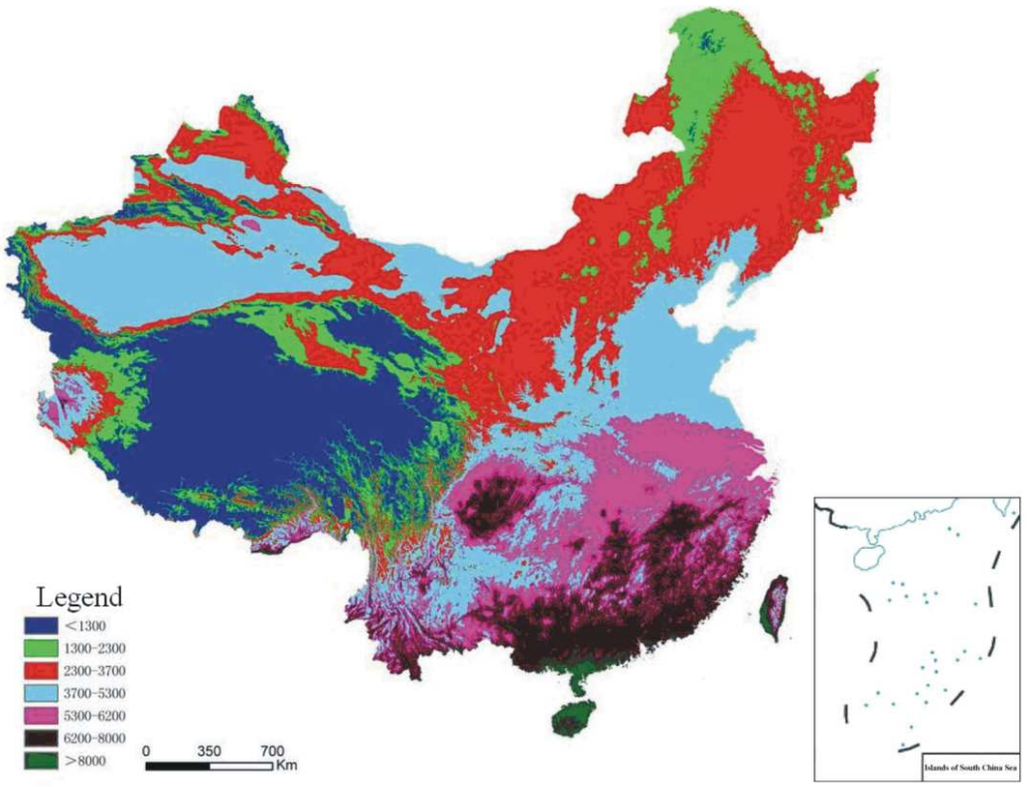

Figure 6. 1km x 1km grid map of China showing spatial distribution of GDD by DEM+ IDS interpolation method. DEM, the Digital Elevation Model; IDS, the inverse distance squared method. The legends show the zones of GDD.

Name of super-class group (biome)	Corresponding class code[a]
Tundra and alpine steppe	I A 1,I B 8, I C 15,I D 22, I E 29, I F 36
Frigid desert	II A 2, III A 3, IV A 4
Semi-desert	II B 9, III B 10, IV B 11, V B 12
Steppe	16IIC,17IIIC,18IV,19VC,25IVD
Temperate humid grassland	IID 23, IIID 24, IIE30
Warm desert	VA 5, VIA 6, VIIA 7
Savanna	VIB 13, VIIB 14, VIC 20, VIIC 21
Forest, including Temperate forest, Sub-tropical forest and Tropical forest	VD 26, VID 27, VIID 28, IIIE 31, IVE 32, VE 33, VIE 34, VIIE 35, IIF 37, IIIF 38, IVF 39,V F40, VIF 41, VIIF 42

[a] The class name refers to Figure7. Explanation

Table 2. The relationships between super-classes (biomes) and classes according to IOCSG approach

http://dx.doi.org/10.5772/57297

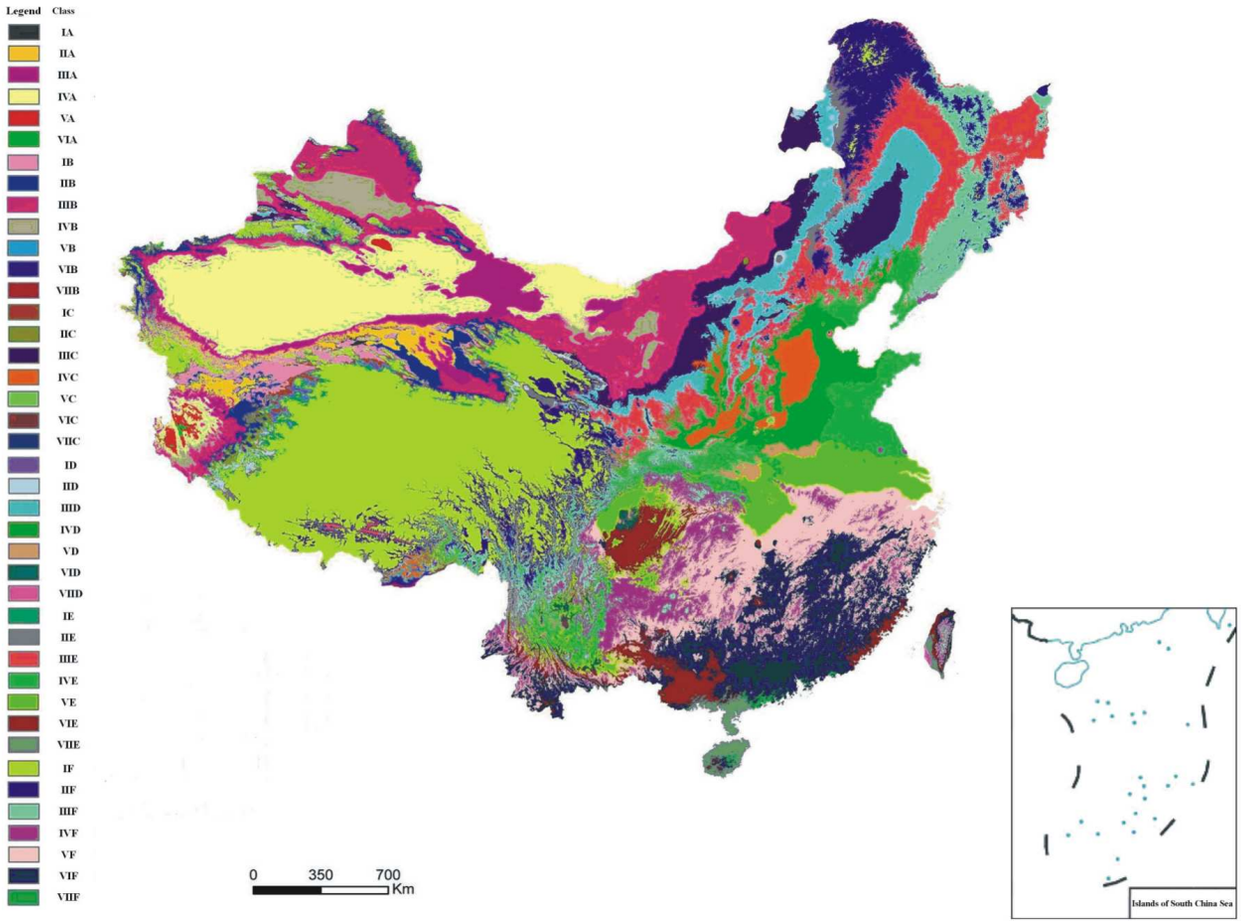

Explanation: IA 1 Frigid-extrarid frigid desert, alpine desert; IIA 2 Cold temperate-extrarid montane desert; IIIA 3 Cool temperate-extrarid temperate zonal desert; IVA 4 Warm temperate-extrarid warm temperate zonal desert; VA 5 Warm-extrarid subtropical desert; VIA 6 Subtropical-extrarid subtropical desert; VIIA 7 Tropical-extrarid tropical desert; IB 8 Frigid-arid frigid zonal semidesert,alpine semidesert; IIB 9 Cold temperate-arid montane semidesert; IIIB 10 Cool temperate-arid temperate zonal semidesert; IVB 11 Warm temperate-arid warm temperate zonal semidesert; VB 12 Warm-arid warm subtropical semidesert; VIB 13 Subtropical arid subtropical desert brush; VIIB 14 Tropical arid tropical desert brush; IC 15 Frigid-semiarid dry tundra,alpine steppe; IIC 16 Cold temperate-semiarid montane steppe; IIIC 17 Cool temperate-semiarid temperate typical steppe; IVC 18 Warm temperate-semiarid warm temperate typical steppe; VC 19 Warm-semiarid subtropical grasses-fruticous steppe; VIC 20 Subtropical-semiarid subtropical brush steppe; VIIC 21 Tropical-semiarid savanna; ID 22 Frigid-subhumid moist tundra,alpine meadow steppe; IID 23 Cold temperate subhumid montane meadow steppe; IIID 24 Cool temperate-subhumid meadow steppe; IVD 25 Warm temperate-subhumid forest steppe; VD 26 Warm-subhumid deciduous broad leaved forest; VID 27 Subtropical-subhumid sclerophyllous forest; VIID 28 Tropical-subhumid tropical xerophytic forest; IE 29 Frigid-humid tundra, alpine meadow; IIE 30 Cold temperate-humid montane meadow; IIIE 31 Cool temperate-humid forest steppe, deciduous broad leaved forest; IVE 32 Warm temperate-humid deciduous broad leaved forest; VE 33 Warm-humid evergreen-deciduous broad leaved forest; VIE 34 Subtropical-humid evergreen broad leaved forest; VIIE 35 Tropical-humid seasonal rain forest; IF 36 Frigid perhumid rain tundra,alpine meadow; IIF 37 Cold temperate perhumid taiga forest; IIIF 38 Cool temperate perhumid mixed coniferous broad leaved forest; IVF 39 Warm temperate perhumid deciduous broad leaved forest; VF 40 Warm-perhumid deciduous-evergreen broad leaved forest; VIF 41 Sub-tropical perhumid evergreen broad leaved forest; VIIF 42 Tropical-perhumid rain forest. The legend above also applies to Table 2)

Figure 7. Map of China showing the spatial distribution of potential class recognized by the IOCSG.

3.2.2. Results

3.2.2.1. Comparison between NPP observations and predictions

Figure 8. plots predicted grassland NPP versus observed NPP values. The results indicate that the Schuur Model underestimated grassland NPP. The Miami Model overestimated the large observations, while the Classification Indices-based Model overestimated as many data points as it underestimated. Considering the slopes and intercepts of the regression of predicted NPP by the Miami Model and Classification Indices-based Model versus observed NPP, the regression of the Miami Model has a slope similar to that of the Classification Indices-based Model (0.79 and 0.72, respectively), but the intercept of the regression line of the Classification Indices-based Model (64.19) is much closer to zero than is that of the Miami Model (113.40). The intercept differences suggest that the Miami Model overestimated the high values of observed NPP, whereas the Classification Indices-based Model slightly underestimated the high values.

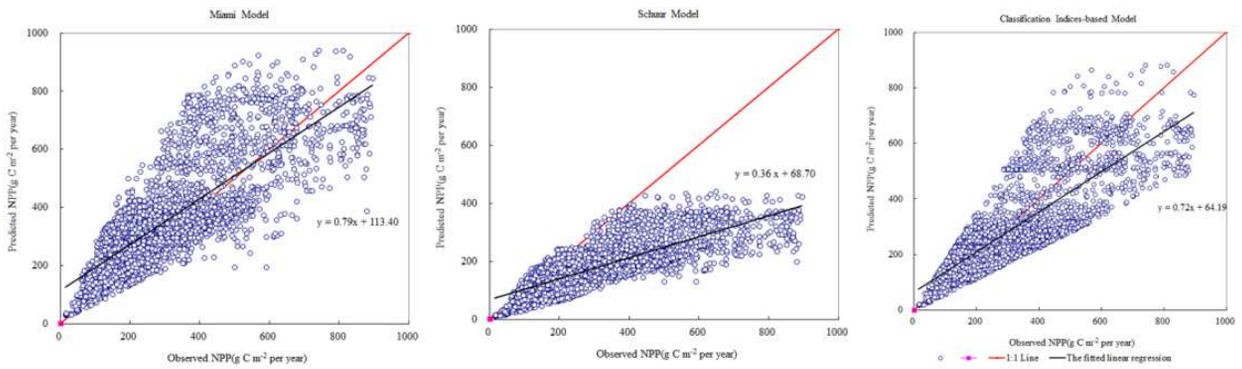

Figure 8. Performance of the Miami, Schuur and Classification Indices-based Models expressed as scatter-plots of predicted versus observed grassland NPP in China.

Comparison of the predicted with the observed grassland NPP indicated that the CVRMSE value using the Classification Indices-based Model was <10%, demonstrating that the prediction of the Classification Indices-based Model is considered excellent, while the output of the Miami Model is considered good, with CVRMSE 13.0%. As the CVRMSE value using the Schuur Model is 23.9%, its predictive ability is considered fair. The results of linear regression showed that the Classification Indices-based Model explained, on average, 65.3% (R^2) of the variation in observed NPP, while the Miami Model explained 63.0% (R^2) of the variation. With the highest E value, the Classification Indices-based Model ranked first for predicting NPP, followed by the Miami and Schuur Models, respectively, indicating that the Classification Indices-based Model can estimate grassland NPP more precisely (Table 3).

3.2.2.2. Distribution patterns of grassland NPP in China

Almost all classes (42 classes) occur in China, except for tropical-extra-arid tropical desert (VIIA7) under current climate conditions (Figure 7). The spatial distribution of grassland

http://dx.doi.org/10.5772/57297

Model	MBE	CVRMSE (%)	R^2	E
Miami Model	102.0	13.0	0.630	0.72
Schuur Model	191.7	23.9	0.629	0.58
Classification Indices-based Model	58.7	9.5	0.653	0.77

Table 3. The mean bias error (MBE), coefficient of variation of the root mean square error (CVRMSE), coefficients of determination (R^2), and model efficiency (E) for the comparison of the predicted with the observed grassland NPP in China.

biomes (Table 2) under current conditions is shown in Figure 9a. The Grassland category was predicted to be distributed primarily in the arid and semi-arid regions of Northern China, the Qinghai-Tibetan Plateau, and scattered throughout warm-temperate and tropical regions (Figure 9a). From north to south, grassland biomes were predicted to be mainly distributed as follows: Tundra and alpine steppe (accounting for 20.42% of Chinese land area); Cold desert (13.1%); Semi-desert (8.1%); Steppe (8.0%); Temperate humid grassland (6.0%); Warm desert (0.1%) and Savanna (0.1%) (Figure 9a and Table 4). These percentages correspond to the actual grassland distribution.

Compared with the Classification Indices-based Model and Miami Model, the Schuur Model estimated substantially lower TNPP, especially in Tundra and alpine steppe, Cold desert, Semi-desert, Steppe, Temperate humid grassland and Savanna areas (Table 4), but the simulated spatial pattern for grassland NPP is very similar (Figure 9b, c, d). Comparing the NPP maps (Figure 9b, c, d) with the data in Table 4 shows highest TNPP of grassland biomes in Tundra and alpine steppe, followed by Steppe and Temperate humid grassland, respectively. The Tundra and alpine steppe, which covers the largest area, was predicted to be mainly distributed in the Tibet Autonomous Region (94.4 million hectares), Qinghai Province (49.1 million hectares) and Xinjiang Uygur Autonomous Region (32.1 million hectares). Although Tundra and alpine steppe has lower NPP values than Temperate humid grassland on a unit area basis, the TNPP for Tundra and alpine steppe, estimated by the Classification Indices-based Model, was predicted to be nearly twice as large as that of Temperate humid grassland because Tundra and alpine steppe was predicted to cover a greater area (Table 4). The total area of Steppe and Temperate humid grassland was predicted to be 130.75 million hectares, accounting for 25.0% of the total grassland area, with nearly half of distributed on the Inner Mongolian Plateau. Savanna and Warm desert super-classes were predicted to cover less than 1.3 million hectares. Savanna was predicted to be located in southern China, particularly in Hainan Province, and Warm desert was predicted to be located in the Tarim Basin in Xinjiang Uygur Autonomous Region and the Qaidam Basin in Qinghai Province (Figure 9a). Warm desert and Savanna were predicted to have the lowest TNPP, and Semi-desert and Cold desert to have moderate TNPP values (Figure 9 and Table 4). The Semi-desert was predicted to be mainly distributed in Xinjiang Uygur Autonomous Region (33.8 million hectares) and Inner Mongolia Autonomous Region (26.4 million hectares). The Cold desert was predicted to be mainly distributed in Xinjiang Uygur Autonomous Region (84.3 million hectares), the western region of Inner Mongolia Autonomous Region (18.7million hectares) and Gansu Province (11.9 million hectares).

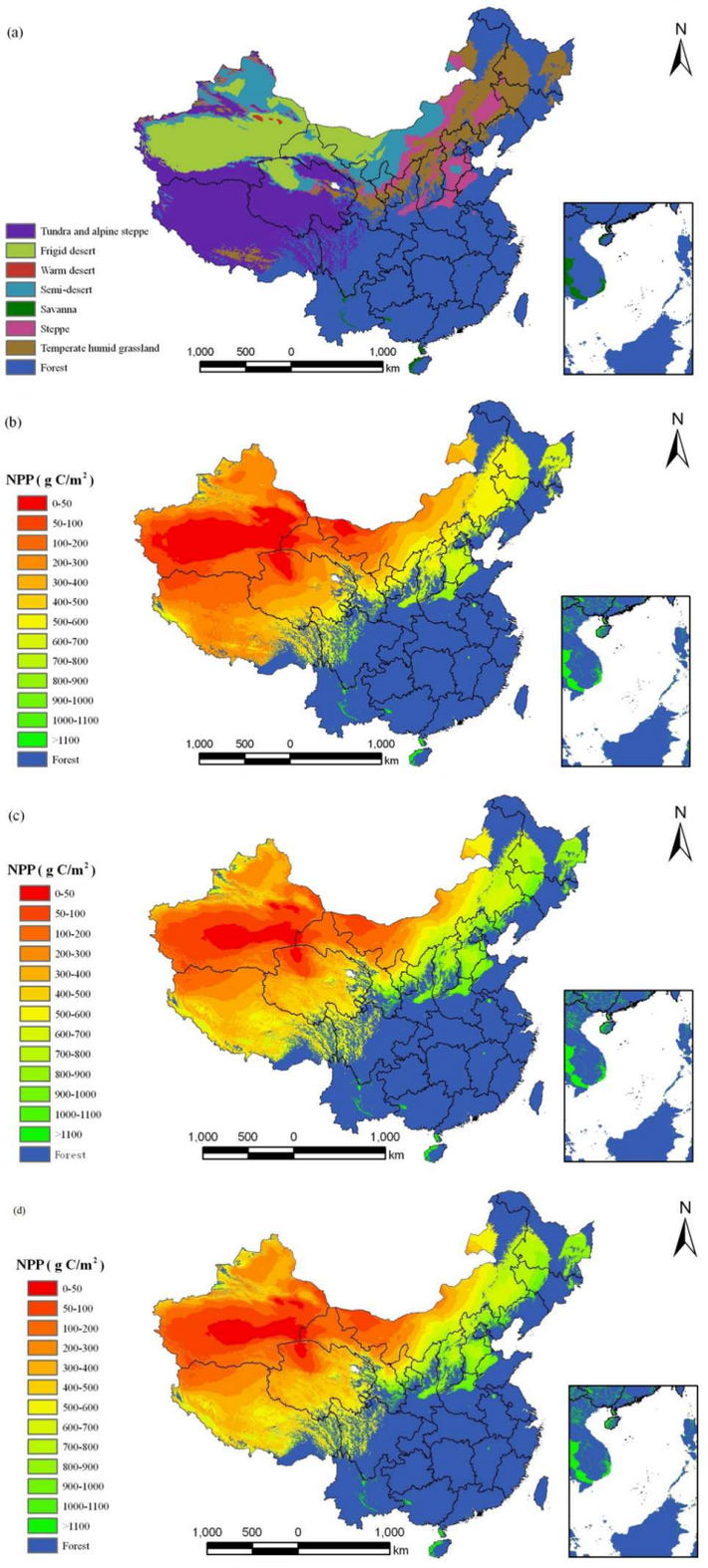

Figure 9. Spatial distribution of (a) potential grassland biomes (super-class group) and (b, c, d) geographical distribution of grassland NPP evaluated by the Miami Model, Schuur Model and Classification Indices-based Model at current climatic condition, respectively.

http://dx.doi.org/10.5772/57297

Biome (super-class group)	Area (million hectares)	TNPP (Tg C)		
		Miami Model	Schuur Model	Classification Indices-based Model
Tundra and alpine steppe	191.47	329.63	184.42	250.70
Cold desert	123.21	52.11	29.15	36.09
Semi-desert	76.19	110.61	61.88	93.68
Steppe	74.99	265.34	148.45	211.65
Temperate humid grassland	55.76	167.86	93.91	124.70
Warm desert	0.80	0.14	0.08	0.04
Savanna	1.25	7.34	4.11	6.71
Forest, including Temperate forest, Sub-tropical forest and Tropical forest	413.65	2529.04	1414.94	2227.83

Table 4. Total NPP (TNPP) of major China's terrestrial biomes estimated by the Miami Model, Schuur Model and Classification Indices-based Model under current climatic condition.

In conclusion, under current climate conditions, the main parts of China's grassland are predicted to be the Tundra and alpine steppe and Steppe, and they account for 50.88% China's total grassland and 63.77-63.90% China's grassland TNPP (Table 4).

3.2.3. Discussion

3.2.3.1. Model-data comparison

The performance of the different models can be compared on the basis of their error frequency distributions. Figure 10 shows the distribution of errors for the three models. Even though the pattern is to some extent controlled by the heterogeneous distribution of the validation points, the direct influence of the different models on the error structure remains evident. In the Miami Model, the error distribution (Figure 10a) shows a unimodal trend with a peak centered on a negative value (average local error of about -48 g C m^{-2} per year) and an error range from -419 to 492 g C m^{-2} per year. The largest underestimated values occur with the Schuur model, although a few overestimated predictions are also present in the same areas. In the histogram of error frequency (Figure 10b), a large single maximum is clearly centered on values of approximately 132 g C m^{-2} per year, indicating that grassland NPP is underestimated almost everywhere within the test area (Figure 8). The fact that the Schuur Model produced a model

efficiency value of 0.58 is an indication that any predictions arising from this model must be treated cautiously. The Classification Indices-based and Miami models have more consistent behavior throughout the validation points, and Figure 10c indicates that the results of the Classification Indices-based Model are in good agreement with observed data (mean error 23 g C m^{-2} per year with a standard deviation of 105.6 g C m^{-2} per year) and the mean absolute error is lower than that obtained from the Miami Model.

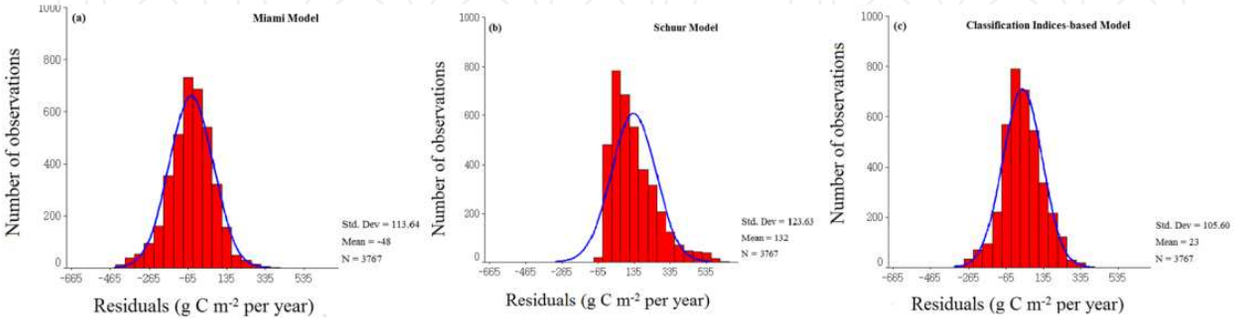

Figure 10. Frequency distribution of residuals for (a) the Miami, (b) the Schuur, and (c) the Classification Indices-based Models. Residuals are expressed as the difference between observed and predicted NPP.

The Classification Indices-based Model performs slightly better than the Miami Model, with a narrower error range and an error histogram that approximates a bell-shaped distribution (Figure 10). In general, the distribution of residuals is homogeneous, although a few larger errors occur in the Classification Indices-based model, which can compromise its reliability. Comparing the Miami Model with the Classification Indices-based Model, the Miami Model determines NPP for a particular location by comparing the minimum value of either temperature or precipitation functions. Hence, it only considers a single factor, and there are no interactions between the two variables. In contrast, the Classification Indices-based Model considers three meteorological measurements and their interactions in its formulation. The reduction in errors produced by the Classification Indices-based Model should lead to significant improvements in applications as a newer NPP-climate relationship model (Figure 10).

3.2.3.2. Grassland carbon budgets

The Classification Indices-based Model has two advantages: 1) it needs few input parameters; and 2) remote sensing data can be incorporated easily. Consequently, the Classification Indices-based Model is effective and practical for large-area application. But the simulated NPP by the Classification Indices-based Model was ideally potential value and land-use practices were not taken into account. The potential grassland, as a final state of succession which achieves the balance with its habitat, is the most stable and mature climax grassland class of the habitat without human interference, and is the trend of the regional grassland development. The study of potential grassland can substantially reveal the impact of climate on the changes of grassland patterns. It is the starting point of the vegetation-environmental

http://dx.doi.org/10.5772/57297

classification and relationship study, as well as the key point of the global change and grassland ecosystem study [27].

The Classification Indices-based Model estimate of China's TNPP at 2.95 Pg C (Table 4) is close to the estimates of 2.65 Pg C and 2.24 Pg C by the light-use efficiency model [48] and the BEPS (Boreal Ecosystem Productivity Simulator) model [49] under current climate conditions, respectively. The Classification Indices-based Model outputs suggest that potential TNPP of grassland in China is 0.72 Pg C under current climate conditions (Table 4). China's grassland TNPP was estimated by Piao et al. [50] as 1.04 Pg C from 1980 to 1988, while Ni [51], using the carbon density method, estimated the TNPP of China's grasslands as 3.06 Pg C between 1949 and1978 and also between 1979 and 1990. This wide range in the reported potential TNPP could be due to their use of different estimation methods, inconsistent classification systems, and/or different time periods with changing grassland areas.

3.2.3.3. Human Appropriation of Net Primary Production (HANPP)

One of the central issues of sustainable development is the question of how to meet the globally growing demand for biomass in an ecologically sound way. Land use activities, primarily for agricultural expansion and economic growth, have transformed one-third to one-half of our planet's land surface from forest or grassland clearance, agricultural practices and urban expansion, which make profound impacts on ecosystem service, food production and the environment [52]. China, occupying only 7% of the world's total arable land, supports nearly 21% of the world's total human population. Agriculture is the major sector of growth in the Chinese economy and with 80% of Chinese living in villages, a large proportion of these people are still dependent upon agriculture. However, with rapid industrialization, urbanization is accelerating and leading to changes in grassland and forest land uses. With increasing scientific and political interest in regional aspects of the global carbon cycle, there is a strong impetus to better understand the carbon balance of China. This is not only because China is the largest emitter of fossil-fuel CO_2 into the atmosphere, but also because it has experienced regionally distinct land-use histories and climate trends, which together control the carbon budget of its ecosystems [53, 54]. Changes in terrestrial ecosystems through human land use and management are also important in land degradation and carbon balance studies. Environmental degradation is a major concern for China and research aimed at understanding the linkages between land use changes, socioeconomics and the biophysical variables governing environmental degradation is needed. Despite the vast amount of research conducted independently on land use changes and social indicators in China, an integrated assessment combining them to study the socioeconomic metabolic flows and their impact on land resources on a large spatial scale is absent. In this context, the concept of HANPP (human appropriation of net primary production) is an important tool for assessing the impact of anthropogenic forces through land use changes on biomass.

HANPP is an indicator of the extent to which ecosystem processes are altered by human activities. HANPP equates to the difference between the NPP of the potential natural vegetation and the amount of NPP remaining in ecosystems. The notion of HANPP represents the food supply for humans, providing the free energy for humans to sustain their metabolic

activities and allowing them to perform physical work. For example, agriculture and forestry harness biomass energy for socio-economic purposes and thereby reduce the amount of NPP remaining in ecological food chains [52, 55-58]. HANPP alters the composition of the atmosphere, levels of biodiversity, energy flows within food webs and the provision of important ecosystem services [59-61]. This removal of carbon naturally comes at a cost in that increased intensities of human appropriation should directly result in less vegetative growth compared to its natural state, if all other factors are held constant, such as nutrient availability. In this study, we present a comprehensive assessment of Chinese HANPP based on vegetation modelling using our model, agricultural and forestry statistics, and geographical information systems data on land use, land cover, and soil degradation that localizes human impact on ecosystems. We find, overall, that the HANPP values suggest that more than 43.2% of the available NPP has already been modified and exploited in China. This value is comparatively higher than the range of global estimates of 20% to 40% for HANPP [62, 63]. Furthermore, compared with HANPP estimates cited for Austria [57, 59], where HANPP declined from 1980 to 1995, HANPP has increased in China. Increases in HANPP may lead to carbon fluxes from biota to the atmosphere, they may contribute to biodiversity loss, and they may result in diminished resilience of ecosystems [62]. As Chinese human population grows and with mounting political interest in increasing GDP, there is likely to be an increased requirement for more agricultural areas and further increases in HANPP over the present value. These analyses suggest policy options for slowing future growth of HANPP. It also offers a means to aid people in using the aforementioned carbon sinks to fulfill China's commitment of reducing greenhouse gases.

3.3. Model-data comparison and modelling the potential net primary productivity of global grassland

Grassland biomes account for 25% of the world's land area and have global significance for climate-carbon feedback [1], containing approximately 30% of global soil carbon stocks [64]. Ranging from the savannas of Africa to the North American prairies and the converted grasslands of Latin America and Southeast Asia, grassland ecosystems support the majority of the world's livestock and large mammals [65], besides playing a very important role in regulating the global carbon cycle and providing meat and milk for human beings.

As one of the most widespread ecosystem types, natural grassland plays a significant but poorly recognized role in the global carbon cycle [1, 2]. In order to effectively manage grassland ecosystems and maintain their sustainability, large-scale analysis and modelling of grassland NPP are needed to develop a better grasp of the spatial distribution of grasslands and their productivity [3, 4, 13, 20, 66]. Continuous monitoring of global grassland productivity has never been possible because of technological limitations. So it is necessary to use computer models, calibrated with existing data, to study the spatial and temporal variations of grassland NPP [3]. Recently, climate-vegetation models have been drawing much attention and have been widely applied internationally [4, 9, 18], having been shown to yield 'reasonable estimates' of global patterns of productivity [4, 9, 14, 16]. The Miami Model [38], Schuur Model [15] and Classification Indices-based Model [22, 24, 25, 27, 28] are examples of these climate-

http://dx.doi.org/10.5772/57297

vegetation models. But model inter-comparison under a consistent classification system simultaneously has not been attempted. In particular, the quantitative and spatial descriptions of global grassland classes and their NPP values have not been reported.

The purpose of this section is: 1) to compare NPP estimated from the Miami Model [38], Schuur Model [15], and the Classification Indices-based Model [22,24,25,27,28] with NPP derived from measurements at 37 sites around the world, to evaluate the applicability and reliability of the Classification Indices-based Model; and 2) to simulate the spatial distribution patterns and associated NPP characteristics of global potential grassland under recent past climate scenario using the IOCSG approach and NPP-climate models.

3.3.1. Data acquisition and methods

3.3.1.1. Observed NPP database

A reference data set (n = 113) of grassland NPP field observations with paired climatic variables was compiled for this study. Total observed NPP data were gathered from the Oak Ridge National Laboratories (ORNL) Net Primary Production database (http://www-eos-dis.ornl.gov/NPP/npp_home. html), and were the sum of aboveground and belowground NPP following standard methods [9]. The grasslands including the Tundra and alpine steppe, Cold desert, Semi-desert, Steppe, Temperate humid grassland, Warm desert and Savanna, or other intensively managed sites were omitted from this study. Locations of sampling sites were plotted using their associated geographic coordinates, as shown in Figure 11.

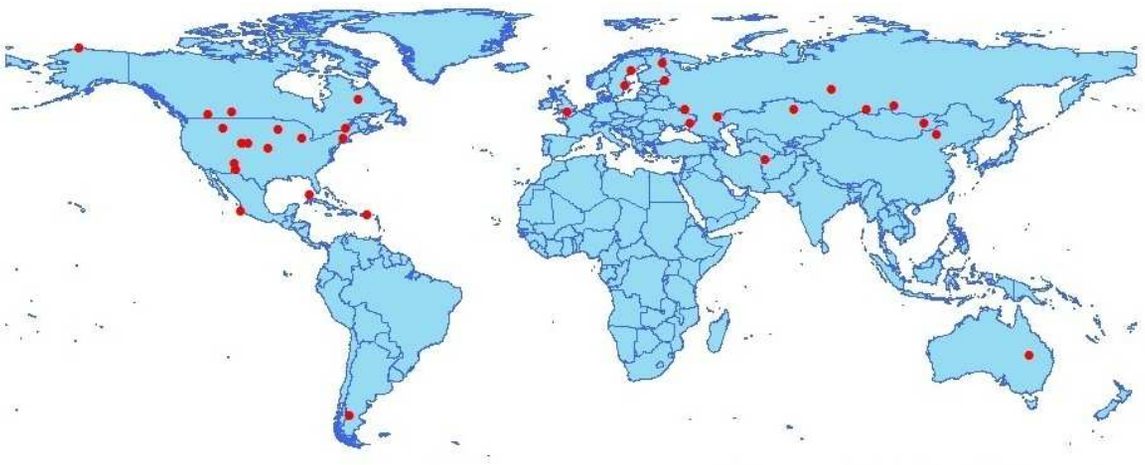

Figure 11. Spatial distribution of grassland NPP observations collected from the ORNL DAAC NPP database (http://www-eosdis.ornl.gov/NPP/npp_home.html).

3.3.1.2. Monthly precipitation and mean temperature grid data

The monthly precipitation and mean temperature grid data, with spatial resolution of 30 arc seconds (i.e., about 1 km), for global land areas excluding Antarctica over 50 years from 1950 to 2000, were generated using the software package ANUSPLIN Version 4.3 (Australian

National University, Canberra, ACT, Australia) [67,68]. We chose this data set because the method that created it has been used in other global studies [69, 70], and it has performed well in comparison with the other multiple interpolation techniques [68, 71].

3.3.1.3. IOCSG approach and NPP-climate model operation

A common approach to extrapolating grassland NPP to the biosphere is to use vegetation maps together with models of plant productivity at a biome level. The IOCSG potential biome maps and its NPP were created and processed by the ArcGIS software (Esri Inc., Redlands, CA, USA) under current climate (1950-2000). In the IOCSG biome (super-class group) classification map, lake water, permanent snow and ice were excluded by using the Moderate Resolution Imaging Spectroradiometer-International Geosphere Biosphere Program (MODIS-IGBP) land-cover classification dataset in 2001, found at http://wist.echo.nasa.gov. The MODIS-IGBP land-cover classification dataset was used to calculate the area of potential grassland biome. The simulated NPP was an ideal potential value, and land-use practices were not taken into account. The total NPP has a unit of Tg C (1 Tg = 10^{12}g) for biome or Pg C (1 Pg = 10^{15}g) for world.

3.3.2. Results

3.3.2.1. Comparison between NPP observations and predictions

Figure 12 plots predicted grassland NPP versus observed NPP values. Data results indicate that the Schuur Model over-predicted grassland NPP. The Miami Model over-predicted the large observations while the Classification Indices-based Model achieved a better balance between over-predicted and under-predicted data points. A 1:1 line fits almost throughout the entire cloud of data points of the Classification Indices-based Model. Considering the slopes and intercepts for the regression of predicted NPP by the three models versus observed NPP, the regression of the Miami Model has a slope (0.77) similar to that (0.70) of the Classification Indices-based Model, but the intercept of the regression line (151.41) of the Classification Indices-based Model is much closer to zero than the regression line (232.52) of the Miami Model. The intercept differences suggested that the Miami Model overestimated the high values of observed NPP, whereas the Classification Indices-based Model slightly underestimated the high values.

Comparison of the predicted with the observed grassland NPP indicated that the CVRMSE value using the Classification Indices-based Model was less than 30%, demonstrating that the prediction suitability of the Classification Indices-based Model is considered fair, while the prediction suitability of the Miami model is considered poor, with the CVRMSE=34.12%. As the CVRMSE value using the Schuur Model is 42.13%, its predictive ability is considered the poorest. The results of linear regression showed that the Classification Indices-based Model explained, on average, a variation of 65.86% (R^2) in observed NPP, while the Miami Model showed the explanations of 59.46% (R^2). With the highest E value, the Classification Indices-based Model ranked first for predicting NPP, indicating that the model can estimate the grassland NPP more precisely (Table 5).

http://dx.doi.org/10.5772/57297

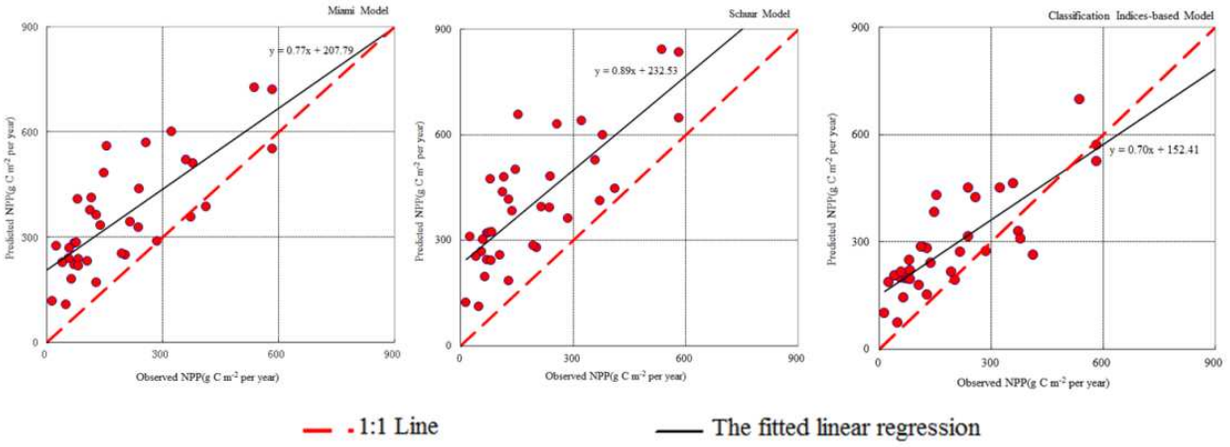

Figure 12. Performance of the Miami, Schuur and Classification Indices-based Models expressed as scatter-plots of predicted versus observed grassland NPP in World.

Model	MBE	CVRMSE (%)	R^2	E
Miami Model	-162.93	34.12	0.5946	-0.11
Schuur Model	-211.46	42.13	0.6116	-0.07
Classification Indices-based Model	-94.92	23.12	0.6586	0.10

Table 5. The MBE, CVRMSE, coefficients of determination (R^2), and model efficiency (E) for the comparison of the predicted with the observed grassland NPP in World.

3.3.2.2. Spatial distribution patterns and characters of grassland biomes over 1950-2000

The spatial distribution of grassland biomes during the period of 1950-2000 is shown in Figure 13a. From Figure 13a, the potential grassland is characterized by a significant distribution pattern in latitudinal and altitudinal directions. From the Equator to the North Pole, grassland biomes were mainly distributed in sequence as follows: (1) Savanna as the largest terrestrial biome, mainly distributed in the east and middle of Africa, Central America and Oceania; (2) Warm desert, mainly distributed in North Africa, North America and the largest part in Asia; (3) Semi-desert and Cold desert, and mixed with Steppe in central Eurasia Continent and southwest of North America, as well as Tundra and alpine steppe in the Tibetan Plateau; (4) Temperate humid grassland, distributed over the entire Eurasian continent, and extending from the east of North America to the west coast with the Pacific Ocean; and (5) Tundra and alpine steppe, mainly distributed in the north of North America, Greenland and the most northerly part of Eurasia. In the Southern Hemisphere, from the Equator to the southernmost edge of Oceania, there are two major zones, including (1) dominated by Savanna, and mixed with a little bit of Steppe, and Warm desert, mainly distributed in the south and middle of Africa, the north and middle of South America, and the south of Southeast Asia and the north of Oceania; (2) dominated by Semi-desert, mainly distributed in southernmost South America, Africa and Oceania. Probably affected by interactions among topography, climate and vegetation, there are more grassland biomes distributed in the east of South American (Figure

13a). Results of statistical analysis indicated that Grassland and Forest covers 55.76% and 44.24% of global land area, respectively (Table 6). Grassland biomes were mainly distributed as follows: Savanna (accounting for 17.19% of global land area); Warm desert (16.29%); Tundra and alpine steppe (6.32%); Semi-desert (6.03%); Steppe (4.83%); Temperate humid grassland (3.86%) and Cold desert (1.25%) (Table 6). These percentages correspond to the actual grassland distribution.

Biome (super-class group)	Area (million hectares)	TNPP(Tg C)		
		Miami Model	Schuur Model	Classification Indices-based Model
Tundra and alpine steppe	827.96	1884.82	2269.96	2492.34
Frigid desert	163.57	120.65	23.87	92.18
Semi-desert	789.81	1576.73	1177.32	1365.04
Steppe	633.15	1706.27	4705.38	1371.51
Temperate humid grassland	505.43	1049.52	7515.71	841.33
Warm desert	2134.27	1516.60	3138.55	1111.00
Savanna	2251.42	8616.21	2536.42	8103.96
Forest, including Temperate forest, Sub-tropical forest and Tropical forest	5795.39	38904.59	40147.86	39128.38

Table 6. Total NPP (TNPP) of major global terrestrial biomes estimated by Miami, Schuur and Classification Indices-based Models in recent past (1950- 2000)

Comparisons with the Classification Indices-based Model and Miami Model, Schuur Model estimated substantially higher TNPP, especially for Temperate humid grassland, Steppe and Warm desert (Table 6), but the simulated spatial pattern for global NPP is very similar (Figure 13bcd). The NPP increases from the South and North poles toward the Equator, corresponding to changes in precipitation and temperature. Comparing the NPP maps (Figure 13bcd) with the Table 6 shows highest TNPP of grassland in Savanna, followed by Tundra and alpine grassland and Steppe, respectively. Although Warm desert grassland covers the second greatest area among grassland super-classes, TNPP for Warm desert grassland is still lower due to lower NPP.

In conclusion, under recent past climate conditions, the main parts of global grassland are the Savanna and Tundra and alpine grassland, which together account for 42.15% of total global grassland area and 63.76-68.91% of global grassland TNPP (Table 6).

http://dx.doi.org/10.5772/57297

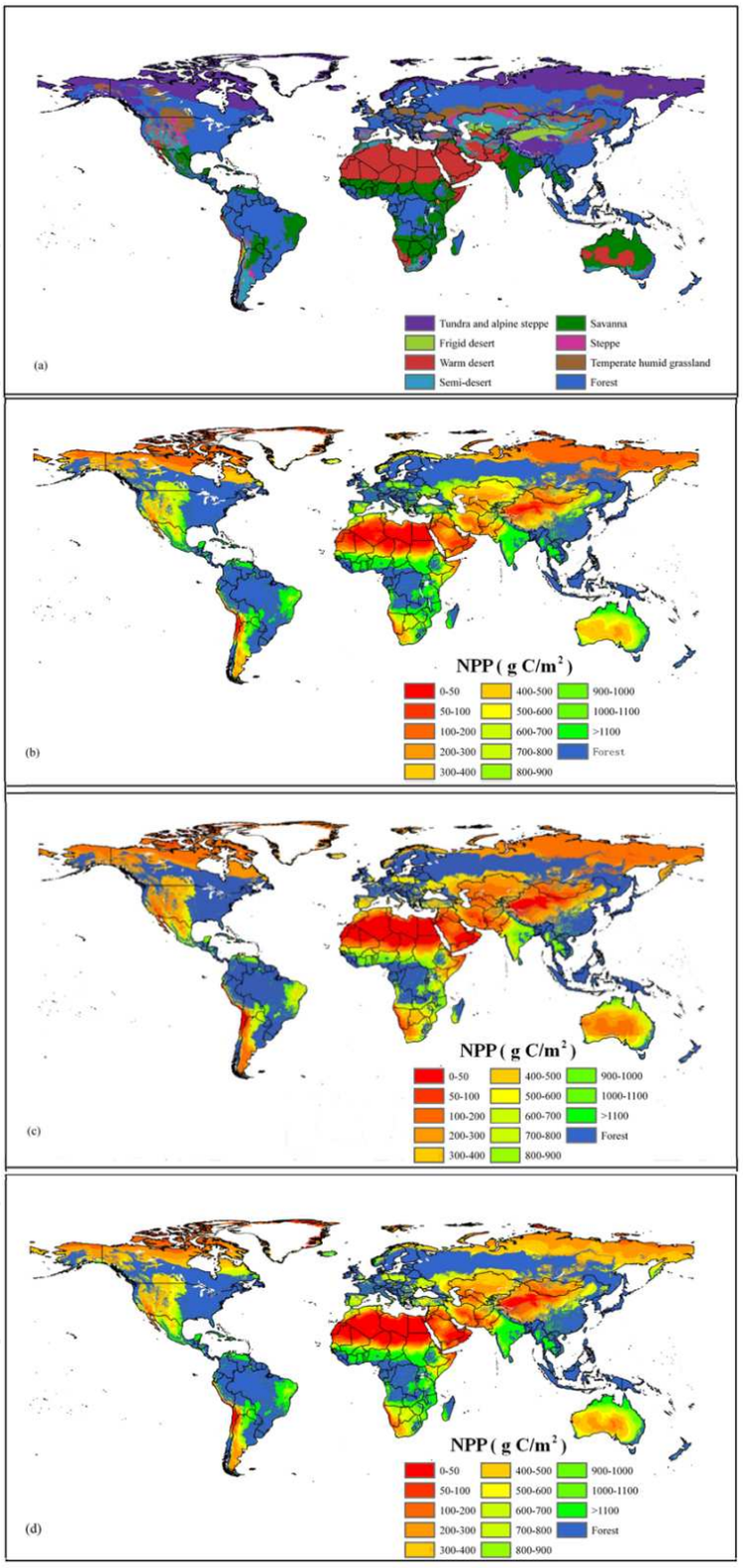

Note: (a) Potential biome (super-class group) classification map; (b, c, d) global pattern of grassland NPP evaluated by the Miami Model, Schuur Model and Classification Indices-based Model.

Figure 13. Global spatial pattern of the potential biome and the grassland NPP for recent past (1950-2000)

3.3.3. Discussion

3.3.3.1. Model-data comparison

GDD, MAP and the moisture index (K value) are used as criteria to determine the class in the IOCSG. The Classification Indices-based Model connected with the IOCSG by using the classification indices as independent variables and considers three meteorological measurements and their interactions in its formulation. The use of these variables allows the Classification Indices-based Model to more accurately predict changes of NPP among grassland classes or super-classes [17, 22, 24, 25, 27, 28]. The model's relative simplicity and ability to make reasonable estimates of the patterns of NPP in global grasslands is attractive. Despite being a newer NPP-climate relationship model, the Classification Indices-based Model provides more accurate conclusions and may also reduce the uncertainty of climate change impacts on grasslands on a global scale. Furthermore, it has the potential to rapidly advance grassland NPP research and application in developing/undeveloped regions or countries that generally lack the detailed and complex data required by other models (i.e., BIOME4).

3.3.3.2. Grassland carbon budgets

The Classification Indices-based Model estimates global TNPP at 54.51 Pg C compared to 55.38 Pg C and 61.52 Pg C using the Miami model and the Schuur Model under recent past climate conditions (Table 6). The Classification Indices-based Model estimate is closer to the estimates of 46 Pg C, 48 Pg C and 55 Pg C by the National Center for Ecological Analysis and Synthesis (NCEAS) model [4], the Carnegie-Ames-Stanford approach (CASA) Biosphere model [72], and the MODIS NPP [73], respectively. This wide range in the reported potential global TNPP could be due to their use of different estimation methods, inconsistent classification systems, and/or different time periods [74]. The potential carbon accumulated in plants was calculated based on simulated NPP. This calculation does not account for the potential impacts from human disturbances, but assumes that the full potential NPP is reached in the grassland. The Classification Indices-based Model estimates global grassland TNPP at 15.38 Pg C compared to 16.47 Pg C and 21.37 Pg C using the Miami model and the Schuur Model under recent past climate conditions (Table 6). Our global-scale NPP estimates can be used to improve understanding of environmental controls on global-scale NPP, help understand how NPP might have been altered by land use [75] and assess the human appropriation of net primary productivity.

4. Grassland in response to climate change

4.1. Introduction

Global climate change will seriously affect terrestrial ecosystems. In global climate change research, modelling is a key method for the study of climate-vegetation, which is an important component in the area of global change research. The current period of climate

http://dx.doi.org/10.5772/57297

change and high CO_2 concentrations in recent years has resulted in warm summers and longer growing seasons, to a change in vegetation patterns can be expected. This change would cause changes in vegetation classes and their NPP. For example, the dominance of some cold-season C_3 grasses would decrease, while that of warm season C_4 grasses could be expected to increase. Global warming also causes changes in precipitation patterns and the total amount of precipitation. The far-reaching consequences of climatic phenomena such as La Niña and El Niño receive widespread attention and appear to be occurring more frequently in recent decades. Zhang et al. [26] recently showed that global warming is already affecting the world's rainfall patterns, bringing more precipitation to northern Europe, Canada and northern Russia, but less to sub-Saharan Africa, southern India and Southeast Asia. They explained that human activity is causing alterations to the water cycle, moving more water vapor away from the warmest parts of the planet and pushing it toward the poles. As a result, wet areas are becoming wetter and dry areas are becoming drier. Thus, there has been an increase in the demand by the broader scientific community and policymakers for better projections of regional impacts of future greenhouse-gas-induced climatic change. Global environmental change, signified by 'global warming' and its possible effects on ecosystems have been drawing increasing attention from the scientists and governments of every country and from all circles of the world [9, 13, 76]. Study of responses of terrestrial NPP to climate changes will help us understand the feedback between climate systems and terrestrial ecosystems and the mechanisms of increased NPP in the northern, middle and high latitudes [77]. NPP is not only used for assessing the carbon balance on regional and global scales, it also plays an important role in demonstrating compliance with the Kyoto Protocol on greenhouse gas reduction [11]. So, accurate estimates of NPP are very important not only for scientifically guiding ecosystem management but also for the study of global climate change [53]. Therefore, study of NPP and its response to global change is one of the key focuses for the global scientific community [9, 78].

Climate change has been identified as having far-reaching implications for the world's grasslands [16, 79-83]. Therefore, understanding the sensitivity of grassland to climate change and the effect of these changes on grassland ecosystems is a key issue in global carbon cycling. NPP in grassland is a key variable in our understanding of carbon exchange between the biosphere and atmosphere, both currently and under climate change conditions [3, 4, 13, 84]. The mechanisms and modelling of responses in grassland NPP to global change will enhance understanding of how grassland ecosystems will respond to global change and the projection of grassland NPP to global change. This will enable the development of countermeasures to maximize the grassland NPP under conditions of global change, especially to provide sustainable development of pasturing in arid and semiarid areas, by using these theoretical and technological methods. The IPCC report [85] states that climate change will present challenges for future grassland use by livestock and other grazers, and for the resulting public policy designed to manage grasslands. Given their vast area and diversity of classes, China's grasslands play an important role in both regional and global carbon cycling [33]. In order to effectively manage grassland ecosystems and maintain their sustainability, a deeper understanding of how these ecosystems will respond to growing

pressures is needed. Large-scale analysis and modelling is needed to develop a better grasp of the spatial distribution of grasslands, their productivity, and potential variations in response to climate changes [3, 4, 13, 20, 23, 66].

Climate change will have profound effects on the class level, which in turn will influence vegetation types and their NPP. Clearly, this requires improved projections of regional climate and understanding of how vegetation types will respond to climate change. Climate is a major driver of variation in NPP, but a clear understanding of the impact of climate change on NPP is lacking [13]. Not only are grassland researchers concerned with the performance of NPP simulation models under contemporary climate, but also they want to know the behavior of these models under extrapolated future environmental conditions [3, 4, 13]. A growing number of research efforts have demonstrated the importance of climate-vegetation interaction in understanding climate sensitivity and climate change [18]. The study of climate-vegetation interaction is the basis for research on terrestrial ecosystems' responses to global change and mainly comprises two important components: climate vegetation classification and NPP of natural vegetation. From the view of generic relationships among all the vegetation types, the IOCSG can be used to predict climate-linked spatial or temporal succession from an original class to a new class as these climatic factors change. Hence, there is potential to develop future scenarios based on possible changes in vegetation type and its NPP in response to climate change in coming years. The IOCSG is a suitable tool to incorporate the effects of both climate change and vegetation management measures on plant growth activity into NPP estimation at the same resolution as satellite data. The Classification Indices-based Model connects with the IOCSG by using the classification indices as independent variables. The use of these variables allows the Classification Indices-based Model to project changes of NPP among grassland classes or super-classes more accurately [17, 22, 24, 25, 27, 28]. The section on Model Validation and Model Inter-comparison has shown that the Classification Indices-based Model is suitable to predict grassland NPP at regional, Chinese or global scale. In addition, the Classification Indices-based Model presented the closest values to the observed in situ meteorological variables. Furthermore, its relative simplicity and ability to generate reasonable patterns of NPP is attractive. Also, GDD and the moisture index (K value) are used as proxies to represent the water and thermal properties of the growing season, and are effective drivers for modelling NPP. The Classification Indices-based Model not only takes into account dynamical classes [17], it also simulates NPP of corresponding classes. As a new NPP-climate relationship model, the Classification Indices-based Model has the potential to evaluate the possible effects of climate change by improving the accuracy of the NPP prediction and reducing the evaluation uncertainty of the possible effects of climate change [22, 24, 25, 27, 28].

In order to effectively model climate change impacts on global grassland distributions and associated NPP, it is important to understand climate dynamics in the recent past (1950-2000) as well as climatic projections for the future (2001-2050). Hence, in this section we: (1) simulate the spatial distribution patterns and associated NPP characteristics of the world's and China's potential grassland under a future climate scenario using the IOCSG

http://dx.doi.org/10.5772/57297

approach and the Classification Indices-based Model; and (2) estimate future trends in response to climate change in the first half of the 21st century by comparing the variation in distribution of NPP with the potential total NPP (TNPP) of grassland between the recent past and the projected future climate scenario. Such findings should improve knowledge about changes in global grassland primary productivity under global warming.

4.2. Data acquisition and methods of analysis

4.2.1. Climate data

Two different global climatic datasets were used in this study. The first was the monthly precipitation and mean temperature grid datasets over 50 years from 1950-2000, described at section of 3.3.1.2. The second dataset was the global monthly precipitation and mean temperature prediction data set (also with 30 arc-second resolution) excluding Antarctica from 2001 to 2050 under the A2a scenario (see below), which was simulated by Australia's Commonwealth Scientific and Industrial Research Organisation (CSIRO) and is available through the website http://www.worldclim.org /futdown.htm [86]. The A2a scenario takes into consideration the following land-use changes: (1) high rate of population growth; (2) slow technological change; and (3) increased energy use, and describes a highly heterogeneous future world in light of regionally-oriented economies. The gridded baseline climate (recent past) and gridded future (2000-2050) A2a climate scenarios were used to estimate changes in mean annual temperature (MAT), growing degree-days (GDD) and mean annual precipitation (MAP).

4.2.2. IOCSG approach and NPP simulation

The IOCSG potential super-class group (biome) maps and its NPP were created and processed by the ArcGIS software (ESRI Inc., Redlands, CA, USA) under the baseline climate (1950-2000) and future climate A2a scenario (2000-2050) on average level. In the IOCSG biome (super-class group) classification map, lake water, permanent snow and ice were excluded by using the Moderate Resolution Imaging Spectroradiometer-International Geosphere Biosphere Program (MODIS-IGBP) land-cover classification dataset in year 2001, found at http://earthdata.nasa.gov. The MODIS-IGBP land-cover classification dataset was used to calculate the area of potential grassland biome. The simulated NPP by the Classification Indices-based Model was an ideal potential value and land-use practices were not taken into account. The recent past map was chosen as a baseline and was used for comparison with projected future climate to estimate trends in changes of class or grassland biome distribution and grassland NPP distribution in response to climate change. Both the IOCSG and the Classification Indices-based Model were applied to analyze the changes in grassland biomes and to measure the change in TNPP of grassland biomes from the recent past (1950-2000) to the future A2a scenario (2001-2050). The total NPP has a unit of Tg C (1 Tg = 10^{12}g) for biome or Pg C (1 Pg = 10^{15}g) for China or the world.

4.3. Modelling global-scale potential grassland changes in spatio-temporal patterns to global climate change

4.3.1. Characteristics of potential grassland over 2001-2050 under A2a scenario

In the A2a scenario, the Savanna, Warm desert, Semi-desert, Tundra and alpine steppe, Steppe, Temperate humid grassland and Cold desert occupy 17.68%, 16.06%, 5.97%, 5.91%, 4.83%, 4.30% and 1.24% of global land area, respectively (Table 7). Table 7 shows the highest TNPP of grassland biomes in the Savanna, followed by Steppe and Semi-desert.

In conclusion, the main grassland biomes found in the world were the Savanna, Steppe and Semi-desert, occupying 50.86% of total global grassland areas and 78.06% of global grassland TNPP under future A2a scenario (Table 7).

Biome (super-class group)	Area (million hectares)	total net primary productivity (TNPP)(Tg C)
Tundra and alpine steppe	774.70	1313.62
Cold desert	162.80	84.76
Semi-desert	782.41	1440.56
Steppe	633.15	1854.16
Temperate humid grassland	563.89	1157.55
Warm desert	2104.30	1235.21
Savanna	2316.12	10197.64
Forest, including Temperate forest, Sub-tropical forest and Tropical forest	5766.10	40389.90

Table 7. TNPP of major global terrestrial biomes estimated by Classification Indices-based Model in future (2001-2050) A2a scenario

4.3.2. Numerical simulations of potential grassland dynamics

Both the IOCSG approach and the Classification Indices-based Model were applied to analyze the succession of classes and super-classes and to measure the change of super-class TNPP from recent past (1950-2000) to future A2a scenario (2001-2050).

4.3.2.1. Change of class and super-class area

The class called Frigid-extrarid frigid desert, alpine desert (IA1), mainly distributed in America and Asia, continuously decreased from recent past to A2a scenario and the rate of decrease per decade was 4.72%. If decreasing rates persist, Frigid-extrarid frigid desert, alpine desert (IA1) could potentially disappear by the second half of this century, while the class called Cold temperate subhumid montane meadow steppe (II D23), mainly distributed in Asia and America, continuously increased from recent past to A2a scenario, by 18.40%.

http://dx.doi.org/10.5772/57297

Climate change also influences the spatial distribution of super-classes. The distribution area for various super-classes in these two time periods shows differing dynamic characteristics from recent past (1950-2000) to future A2a scenario (2001-2050) (Tables 6 and 7). The area of Tundra and alpine steppe will decrease by 53.26 million hectares compared with its size during 1950-2000. Likewise, Warm desert will decrease by 29.97 million hectares. However, trends show that Savanna and Temperate humid grassland will strongly increase, to nearly 123.16 million hectares. Overall, the Forest category will decrease by 29.29 million hectares (Tables 6 and 7).

4.3.2.2. Shift trend of super-classes

The A2a scenario predicts changes in global temperature and rainfall patterns, making wet areas wetter, and dry areas drier (Figure 14), resulting in class conversions from an original class to a new class due to changes in climate conditions. For example, the Frigid perhumid rain tundra, alpine meadow (IF36) class will change to Cold temperate-humid montane meadow (IIE30) with climate warming, or Cold temperate perhumid taiga forest (IIF37) with climate drying. The conversion of classes from recent past to future A2a scenario will result in changes in area and TNPP distribution patterns among biomes (Table 8 and Figure 15a). For example, in the super-class of Tundra and alpine steppe, an area of 656.09 million hectares will be converted to Forest (Legend 18 in Figure 15a and Table 8) in this long-run sequence, which will mainly take place in Asia (accounting for 58.96%) and America (32.21%), while another 182.92 million hectares will be converted to Temperate humid grassland (Legend 15 in Figure 15a and Table 8), a change that will mainly take place in Asia (65.90%). An area of 590.06 million hectares of Forest under recent past climate conditions will be converted into the Temperate humid grassland under A2a scenario (Legend 85 in Figure 15a and Table 8), mainly taking place in Asia (51.14%), the Americas (26.22%) and Europe (22.58%). An area of 389.29 million hectares of Forest will be converted into Savanna (Legend 87 in Figure 15a and Table 8), mainly taking place in the Americas (49.62%) and Africa (35.52%). An area of 253.28 million hectares of Temperate humid grassland under recent past climate conditions will be converted into Steppe under the A2a scenario (Legend 54 in Figure 15a and Table 8), mainly taking place in Asia (48.76%), the Americas (28.89%) and Europe (22.22%). An area of 243.37 million hectares of Steppe will be converted into Semi-desert (Legend 43 in Figure 15a and Table 8), mainly taking place in Asia (49.72%) (Table 8).

An area of 856.54 million hectares of Grassland category will be converted to Forest category and an area of 1089.77 million hectares of Forest category will be converted into Grassland category (Figure 15b. and Table 8). There is a clear increasing trend in the Grassland category. As a whole, areas of Grassland category will increase by 31.76 million hectares, while areas of Forest category will decrease by 29.29 million hectares. The relative area of Grassland category will increase by 0.43% over this period (1950-2050), whereas the relative area of Forest category will decrease by 0.51% over the same period (Tables 6 and 7).

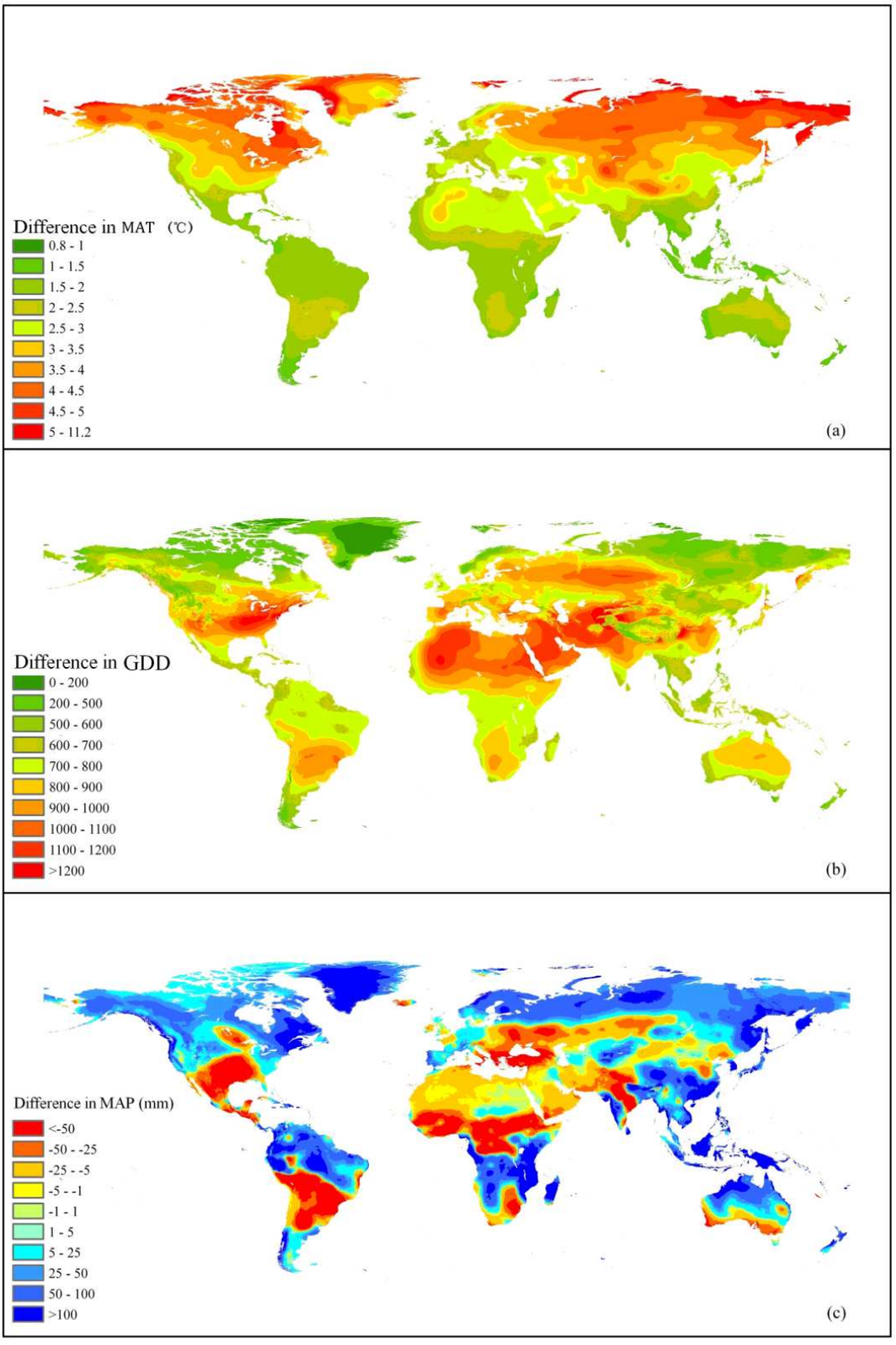

Figure 14. Maps of anomalies in future A2a climatic scenario (relative to the average for 1950-2000) for (a) mean annual temperature (MAT), (b) growing degree-days (GDD) and (c) mean annual precipitation (MAP).

http://dx.doi.org/10.5772/57297

Code	World	Oceania	America	Asia	Africa	Europe
11	774.7	0.06	492.08	305.36	0.01	25.75
12	3.94	-	1.33	2.61	-	-
13	19.89	-	3.20	16.69	-	-
14	13.68	-	1.69	11.98	-	-
15	182.92	-	62.38	120.54	-	-
18	656.09	0.26	211.34	386.85	0.01	57.63
22	108.13	-	12.91	95.21	0.01	-
26	102.80	-	8.26	93.78	0.76	-
32	57.91	-	13.03	44.87	0.01	-
33	502.10	4.51	154.74	299.02	14.40	29.42
34	0.01	-	0.01	-	-	-
36	39.93	0.64	7.80	26.45	5.03	-
37	193.86	43.51	51.26	44.29	38.44	16.35
43	243.37	4.17	65.53	121.01	3.77	48.89
44	70.67	2.27	31.85	28.68	1.94	5.92
47	69.29	6.22	25.44	7.23	13.10	17.30
48	0.20	-	0.07	-	0.13	-
53	29.17	-	2.96	21.38	-	4.83
54	253.28	0.07	73.16	123.50	0.28	56.27
55	290.36	0.11	116.84	158.83	0.01	14.56
58	159.59	0.92	26.57	29.96	0.63	101.51
66	1871.47	168.27	60.84	523.87	1118.23	0.27
67	31.94	25.78	0.21	0.93	5.01	-
76	102.28	20.06	14.40	20.87	46.91	0.03
77	2209.36	427.04	472.40	305.72	993.60	10.61
78	40.66	1.75	0.43	1.90	36.57	-
83	4.18	-	1.93	0.03	0.02	2.20
84	106.24	5.54	18.10	21.51	6.41	54.68
85	590.06	0.18	154.71	301.77	0.18	133.23
87	389.29	7.38	193.16	42.58	138.27	7.90
88	4255.05	84.89	1895.38	1204.96	578.05	491.76

Note: the two digits in the code represents the biome conversion, where the first number depicts the biome under recent past climatic conditions and the second number is under A2a scenario; numbers 1-8 represent Tundra and alpine steppe, cold desert, Semi-desert, Steppe, Temperate humid grassland, Warm desert, Savanna, and Forest, respectively. For example, Code 18 means Tundra and alpine Steppe under recent past climatic conditions would convert into forest in A2a scenario. The number in table is the area of conversion in unit of million hectares.

Table 8. The global biomes conversion matrix from recent past (1950-2000) to future (2001-2050) A2a scenario

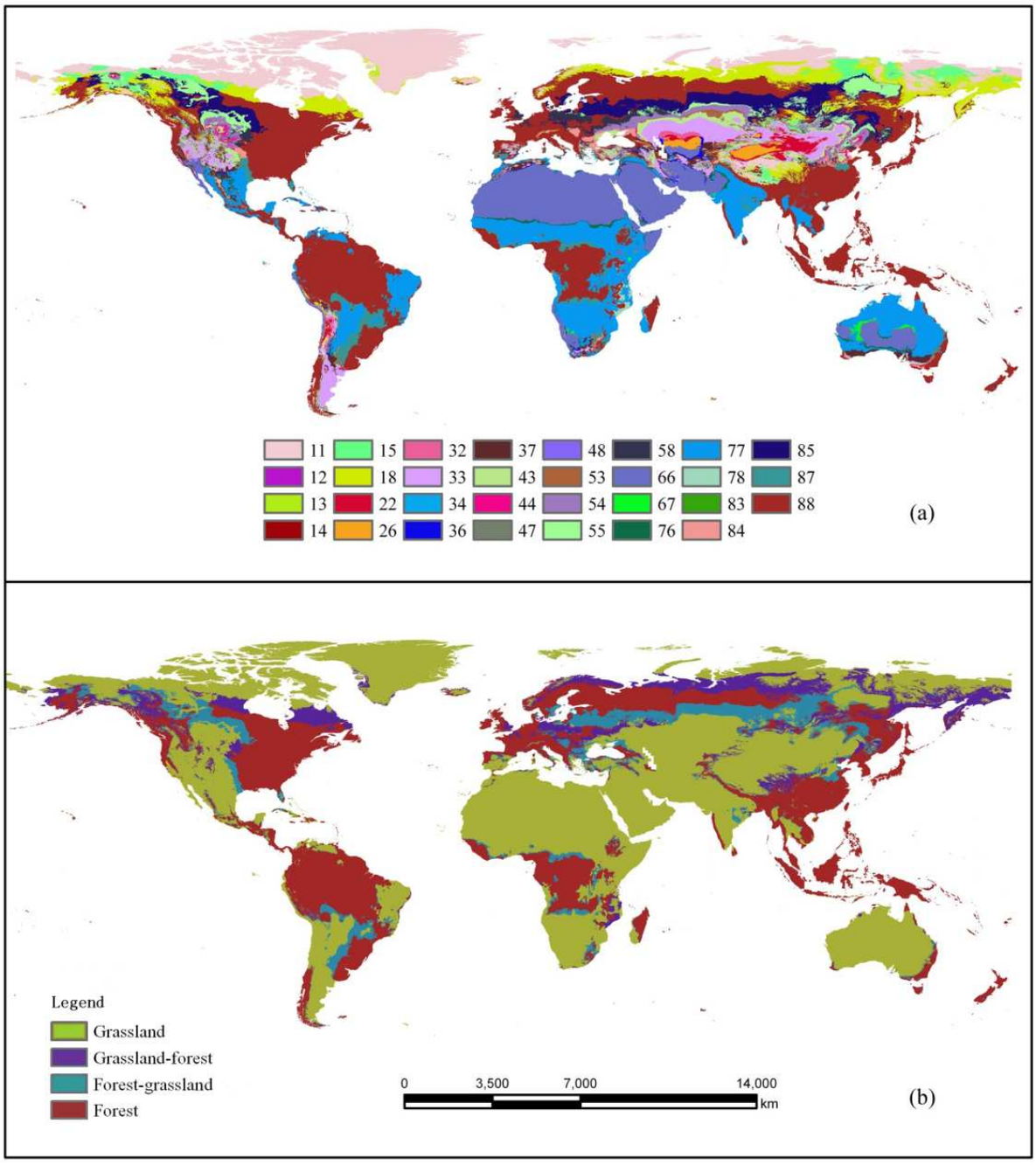

Note: (a) biomes shift. In the legend, the two digits represent the biomes conversion, where the first number depicts the biome under recent past climatic conditions and the second number is under A2a scenario. The numbers 1-8 represent Tundra and alpine steppe, Cold desert, Semi-desert, Steppe, Temperate humid grassland, Warm desert, Savanna, and Forest, respectively. For example, Legend 54 means Temperate humid grassland under the recent past climatic conditions would convert into Steppe under the A2a scenario. (b) Grassland (including Tundra and alpine steppe, Cold desert, Semi-desert, Steppe, Temperate humid grassland, Warm desert, and Savanna) and Forest (including Temperate forest, Sub-tropical forest, and Tropical forest) categories change: Grassland–forest means Grassland category would be converted into the Forest category, Forest-grassland means the Forest category would be converted into the Grassland category; the others are no change.

Figure 15. Spatial distribution dynamics of global potential biomes from recent past to future A2a scenario.

http://dx.doi.org/10.5772/57297

4.3.2.3. Change of TNPP

The Classification Indices-based Model shows NPP either neutral or increasing for most global grid cells during the periods from recent past to A2a scenario (Figure 16).

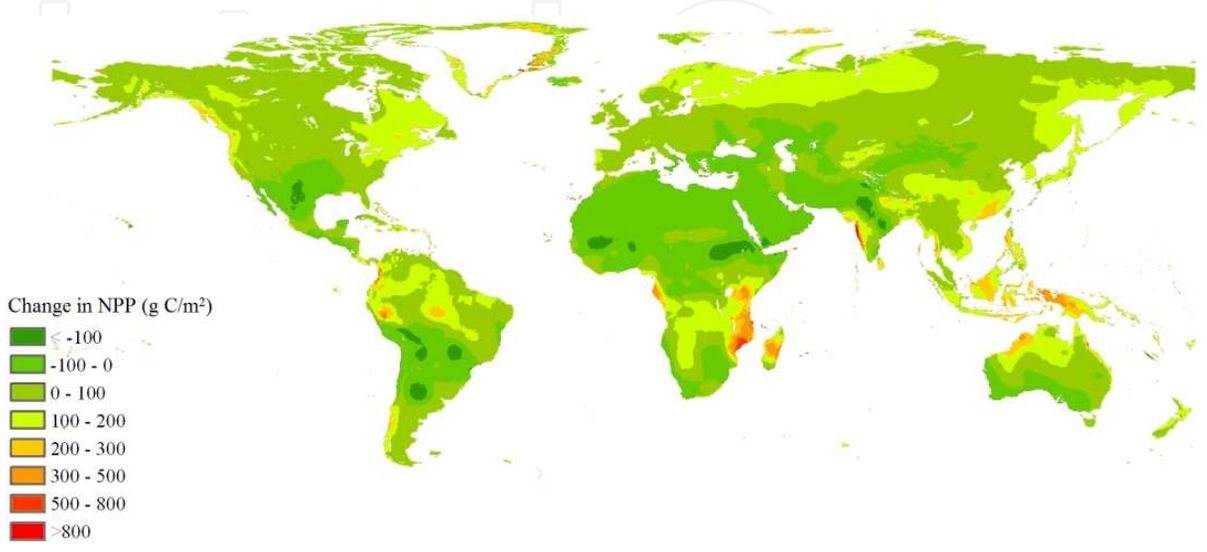

Note: The legends show the differentiated NPP and negative values indicate C loss for NPP.

Figure 16. Trends in global NPP anomalies from 1950 to 2050 computed by the Classification Indices-based Model.

At the class level, the largest increases are in Tropical-humid seasonal rain forest (VIIE 35), Tropical arid tropical desert brush (VIIB14), Tropical-subhumid tropical xerophytic forest (VIID28) and Tropical-semiarid savanna (VIIC 21), as a result of increased MAT and MAP in Africa and the Americas, while TNPP of Frigid perhumid rain tundra, alpine meadow (IF 36), Cold temperate perhumid taiga forest (IIF 37), Sub-tropical perhumid evergreen broad leaved forest (VIF 41), Warm-perhumid deciduous-evergreen broad leaved forest (VF 40), Warm temperate perhumid deciduous broad leaved forest (IVF 39), and Subtropical-subhumid sclerophyllous forest (VID27) decrease sharply. The TNPP of Subtropical-semiarid subtropical brush steppe (VIC20) in Africa shows a marked decrease due to decreased precipitation (Table 9).

At the super-class level, the TNPP of Savanna shows the largest increase, followed by Steppe, Temperate humid grassland, Warm desert and Semi-desert. These increases in TNPP are 2093.68 Tg C, 482.65 Tg C, 316.22 Tg C, 124.21 Tg C and 75.52 Tg C, respectively. The TNPP of Tundra and alpine steppe shows the largest decrease. The simulated TNPP of Tundra and alpine steppe will decrease by 1178.72 Tg C compared with its size during 1950-2000. The decrease of TNPP for Cold desert will be 7.42 Tg C (Table 9).

At the category level, the TNPP of Grassland category will increase 12.40% to 1906.14 Tg C over this period (1950-2050) (Tables 6, 7 and 9).

Biome (super-class group)	Class-ID	Global		Asia		Europe		Africa		America		Oceania	
		Current	A2a	Current	A2a	Current	A2a	Current	A2a	Current	A2a	Current	A2a
Tundra and alpine steppe	IA1	0.02	0.96	0.01	0.23	-	0.07	-	0.05	0.01	0.46	-	0.15
	IB8	5.47	6.82	4.35	6.38	-	-	-	-	1.12	0.44	-	-
	IC15	4.77	5.58	4.04	4.46	-	-	-	-	0.74	1.13	-	-
	ID22	7.10	12.38	6.15	5.95	-	-	-	-	0.95	6.44	-	-
	IE29	38.79	70.51	27.49	34.69	-	-	-	-	11.30	35.83	-	-
	IF36	2436.19	1217.36	1249.53	433.86	215.92	71.70	0.12	0.04	967.04	710.92	3.58	0.84
Frigid desert	IIA2	2.51	1.77	1.81	1.06	-	-	-	-	0.70	0.71	-	-
	IIIA3	23.32	15.78	21.16	12.20	-	-	-	-	2.16	3.58	-	-
	IVA4	66.35	67.21	60.71	59.96	-	-	0.54	0.01	5.10	7.24	-	-
Semi-desert	IIB9	26.13	21.89	19.38	18.90	-	-	-	-	6.75	3.00	-	-
	IIIB10	357.26	276.52	263.64	214.83	1.75	3.90	-	-	91.88	57.78	-	-
	IVB11	470.08	762.99	218.25	400.46	56.49	134.40	35.45	3.53	158.16	224.59	1.73	-
	VB12	511.56	379.16	88.41	104.32	37.32	56.06	98.73	41.67	161.61	151.16	125.50	25.94
Steppe	IIC16	27.93	26.26	22.02	21.05	-	-	-	-	5.91	5.20	-	-
	IIIC17	363.16	312.94	203.41	194.63	33.32	9.36	0.07	-	126.35	108.94	0.01	-
	IVC18	308.63	611.41	85.69	162.77	111.39	284.52	17.09	5.38	84.42	156.78	10.04	1.97
	VC19	271.69	235.16	16.99	60.69	62.59	65.19	52.30	27.77	103.17	53.83	36.64	27.69
	IVD25	400.10	668.39	96.81	105.43	178.71	423.78	23.22	6.62	75.78	119.67	25.59	12.90
Temperate humid grassland	IID23	53.99	101.44	43.96	60.01	-	-	-	-	10.03	41.44	-	-
	IIID24	460.59	573.19	193.04	342.42	90.80	64.68	0.67	0.02	175.48	166.03	0.60	0.05
	IIE30	326.75	482.92	218.82	338.35	0.25	-	-	-	107.68	144.57	-	-
Warm desert	VA5	56.55	52.91	42.65	44.25	-	-	7.83	1.50	6.07	7.17	-	-
	VIA6	351.22	265.31	97.70	109.45	0.25	0.22	96.29	56.62	24.16	31.20	132.82	67.82
	VIIA7	703.24	916.99	212.04	248.00	-	0.03	336.03	420.98	9.29	32.51	145.87	215.47
Savanna	VIB13	1367.24	1337.50	77.23	140.47	19.07	106.51	566.23	342.92	288.82	408.11	415.89	339.49
	VIIB14	3357.22	4848.10	487.68	655.00	-	1.38	1685.12	2316.33	476.02	780.40	708.40	1094.98
	VIC20	714.88	573.17	16.79	75.25	18.77	74.33	372.22	167.42	215.48	204.94	91.63	51.23
	VIIC21	2664.61	3438.87	533.02	629.19	-	0.11	1355.63	1592.66	581.57	973.80	194.40	243.12
Forest, including temperate forest, Sub-tropical forest and tropical forest	VD26	275.02	252.60	65.16	46.27	30.99	70.36	52.70	20.71	99.26	78.71	26.91	36.56
	VID27	768.75	569.52	32.99	136.59	7.98	23.34	438.75	157.32	260.74	229.46	28.30	22.82
	VID28	2991.91	4141.40	668.94	674.43	-	-	1187.64	1629.08	973.51	1643.08	161.82	194.82
	IIIE31	846.52	1313.47	232.00	549.65	433.70	411.61	2.20	0.63	175.74	350.61	2.88	0.96
	IVE32	628.69	860.05	125.12	116.91	257.76	383.06	27.15	8.52	160.99	319.82	57.68	31.74
	VE33	475.38	488.95	211.14	79.74	19.27	63.57	45.45	20.42	176.58	293.46	22.94	31.75
	VIE34	1876.90	1763.09	279.98	419.33	2.34	7.47	785.68	310.50	780.53	993.43	28.38	32.35
	VIIE35	6155.32	7697.00	912.79	1054.92	-	-	2556.00	3506.24	2617.13	3036.96	69.40	98.88
	IIF37	3558.44	2714.89	1447.30	1357.99	658.84	320.88	1.54	0.27	1424.26	1022.19	26.50	13.56
	IIIF38	2575.79	2967.37	466.08	798.74	1064.25	868.80	9.44	4.09	946.25	1233.80	89.76	61.93

http://dx.doi.org/10.5772/57297

Biome (super-class group)	Class-ID	Global		Asia		Europe		Africa		America		Oceania	
		Current	A2a	Current	A2a	Current	A2a	Current	A2a	Current	A2a	Current	A2a
	IVF39	1611.53	1384.49	475.71	356.44	172.41	242.06	44.36	13.16	784.34	634.75	134.71	138.09
	VF40	1094.95	565.79	526.52	298.72	7.25	36.75	73.45	28.14	466.20	168.82	21.53	33.35
	VIF41	2723.58	1889.94	1288.70	1161.66	-	4.23	294.95	194.80	1109.11	511.00	30.82	18.25
	VIIF42	13545.59	13781.35	4329.50	5041.14	-	-	1507.98	1158.16	7621.36	7475.14	86.74	106.92

Note: The class name refers to Figure 7 Explanation.Unit of TNPP is TgC.

Table 9. Comparison of TNPP of biomes and classes estimated by the Classification Indices-based Model under the baseline climate (recent past (1950-2000)) and those under future (2000-2050) climatic scenario (A2a)

4.3.3. Discussion

4.3.3.1. Biome conversions

The changing climate will affect the growth of plants, alter the species composition of plant communities and ultimately change community structure [87]. Under these conditions, the classes will shift [3,5] and result in biome conversions [3,5]. Our analysis indicated that Steppe will experience the largest variation in biome conversions. The result is the same as the conclusion of Liu et al. [88], who confirmed that under climate warming, the temperate steppe in the arid and semiarid regions of northern China will act as a net C source. The Savanna and Temperate humid grassland will have the highest percentage of growth. The Tundra and alpine steppe biome will have the greatest change in total area, followed by Forest (Tables 6, 7 and 9).

4.3.3.2. Trends in grassland NPP in response to climate change

The Classification Indices-based Model estimates global potential grassland TNPP at 16.47 Pg C and global TNPP at 57.67 Pg C under future climatic A2a scenario (Table 7). Climate change is expected to affect the TNPP of grassland. Understanding climate and NPP feedback cycles in grasslands requires knowledge of the changes in spatial patterns on the NPP of grasslands. The dynamic change characteristics of potential biomes (Table 8 and Figure 15) reflect further evidence of increasing global warming since the early 1980s (Intergovernmental Panel on Climate Change, 2007). The Classification Indices-based Model estimated an increase of 1.09 Pg C in TNPP for global potential grassland from recent past to future A2a scenario (Tables 6, 7 and 9). It will bring an increase of 3.91 Pg in annual sequestration of CO_2 and 2.88 Pg of annual contribution to the atmospheric O_2 cycle respectively (1.63 g of CO_2 is absorbed and 1.2 g of O_2 is released to generate 1 g of DM according to photosynthesis stoichiometry; [89]), which will impose a new issue for future grassland research to support sustainable development and to provide relevant knowledge to meet the challenge of climate change [90].

4.4. Spatio-temporal dynamics on the distribution, extent and NPP of potential grassland in response to climate changes in China

4.4.1. Characters of potential grassland over 2001-2050 under A2a scenario

In the A2a scenario, the Tundra and alpine steppe, Cold desert, Semi-desert, Steppe, Temperate humid grassland, Warm desert, and Savanna were projected to occupy 8.9%, 8.8%, 11.1%, 12.0%, 5.9%, 6.2%, and 1.8% of land area of China, respectively (Table 10). Under scenario A2a, the Classification Indices-based Model projected the highest TNPP to be in the Forest category. Table 10 shows that the highest TNPP values of grassland biomes were projected to be in the Steppe, followed by Semi-desert, Tundra and alpine steppe, and Temperate humid grassland, respectively. In conclusion, it was projected that the two main grassland biomes found in China will be in the Steppe and Semi-desert, and they will occupy 42.2% of China's total grassland areas and 58.3% of China's Grassland TNPP in the future climatic A2a scenario (Table 10).

4.4.2. Comparing the area and TNPP of China's major terrestrial biomes of 1950-2000 with those of 2001-2050 under the A2a scenario

Climate change was projected to influence the spatial distribution of grassland biomes, with a combined distribution ranging from the northeastern plain adjacent to Mongolia to the southern Tibetan Plateau, with warm desert showing the greatest discrepancies. The distribution of the area for various grassland biomes in these two time periods was projected to change considerably from the recent past (1950-2000) (Table 4) to the future (2001-2050) in the A2a scenario (Table 10). The area of Tundra and alpine steppe was projected to decrease by 107.9 m ha compared with its size during 1950-2000. The TNPP of Tundra and alpine steppe was projected to change from 250.7 to114.0 Tg C. This is a huge reduction of 54.5% due to global climate change. Likewise, the areas of the Cold desert and Temperate humid grassland were projected to decrease by 40.9 and 0.5 m ha, respectively, while the TNPPs of the Cold desert and Temperate humid grassland were projected to decrease by 1.4 Tg C and 14.1 Tg C, respectively. The Warm desert and Savanna super-class groups were projected to increase the most. The area of Warm desert, Steppe, Semi-desert, and Savanna were projected to increase considerably, by nearly 138.2 m ha (Tables 4 and 10).

4.4.3. Numerical simulations on potential grassland dynamics

4.4.3.1. Changes in class

The changing climate is likely to affect the growth of plants, alter the species composition of plant communities, and ultimately change plant community structure [87]. It is anticipated that the classes will shift [3, 5] and will result in biome conversions. Under the A2a scenario, a new class (sub-tropical-extra-arid sub-tropical desert, VIA6) was projected to appear in conjunction with climate warming and drying, and this would be distributed in the Xinjiang Uygur Autonomous Region. The class called Frigid per-humid rain tundra, alpine meadow (IF 36), mainly distributed in the Tibetan Plateau, is projected to decrease continuously under the A2a scenario, with a rate of decrease per decade of 6.8%. If such rates persist, Frigid per-

http://dx.doi.org/10.5772/57297

Biome(super-class group)	Area(million hectares)	TNPP (Tg C)
		Classification Indices-based Model
Tundra and alpine steppe	83.54	114.02
Cold desert	82.36	34.68
Semi-desert	103.66	163.53
Steppe	112.38	318.95
Temperate humid grassland	55.23	110.58
Warm desert	58.41	11.03
Savanna	16.97	75.49
Forest, including Temperate forest, Sub-tropical forest and Tropical forest	424.97	2455.82

Table 10. TNPP of major China's terrestrial biomes estimated by the Classification Indices-based Model from 2001 to 2050 under A2a scenario

humid rain tundra, alpine meadow (IF 36) could potentially disappear by the end of the century.

4.4.3.2. Trends in super-classes

The A2a scenario projects changes in China's temperature and rainfall patterns, making wet areas wetter and dry areas drier (Figure 17), resulting in class succession from an original class to a new class if one just considers changes in climate conditions. The model outputs suggest that the conversion of classes from the recent past to the A2a scenario would result in changes in distribution patterns of the area and TNPP among biomes. Table 11 showed the projected results of the changes in areas of biome conversions between the recent past and the future climatic A2a scenario. For example, in this long time sequence, an area of 58.0 million hectares of Tundra and alpine steppe would be converted to Forest (Legend 18 in Figure 18a and Table 11), which would take place mainly in the Tibet Autonomous Region (accounting for 40.1% of the change) and Qinghai Province (35.9% of change), while another 28.9 million hectares would change to Temperate humid grassland (Legend 15 in Figure 18a and Table 11), and this change would mainly take place in the Tibet Autonomous Region (78.1%). Likewise, an area of 56.9 million hectares of Cold desert under recent climate conditions would be converted into Warm desert under the A2a scenario (Legend 26 in Figure 18a and Table 11), mainly taking place in the Xinjiang Uygur Autonomous Region (99.1%). An area of 43.7 million hectares of Temperate humid grassland would be converted into Steppe (Legend 54 in Figure 18a and Table 11), mainly taking place in the Inner Mongolia Autonomous Region (42.5%). An area of 36.3 million hectares of Forest under recent climate conditions would be converted into Temperate humid grassland under the A2a scenario (Legend 85 in Figure 18a and Table 11), mainly taking place in both Heilongjiang Province (38.9%) and Inner Mongolia Autonomous Region (29.3%), respectively. There would be an area of 28.5 million hectares of Steppe changing to Semi-desert

(Legend 43 in Figure 18a and Table 11), mainly taking place at the Inner Mongolia Autonomous Region (44.8%).

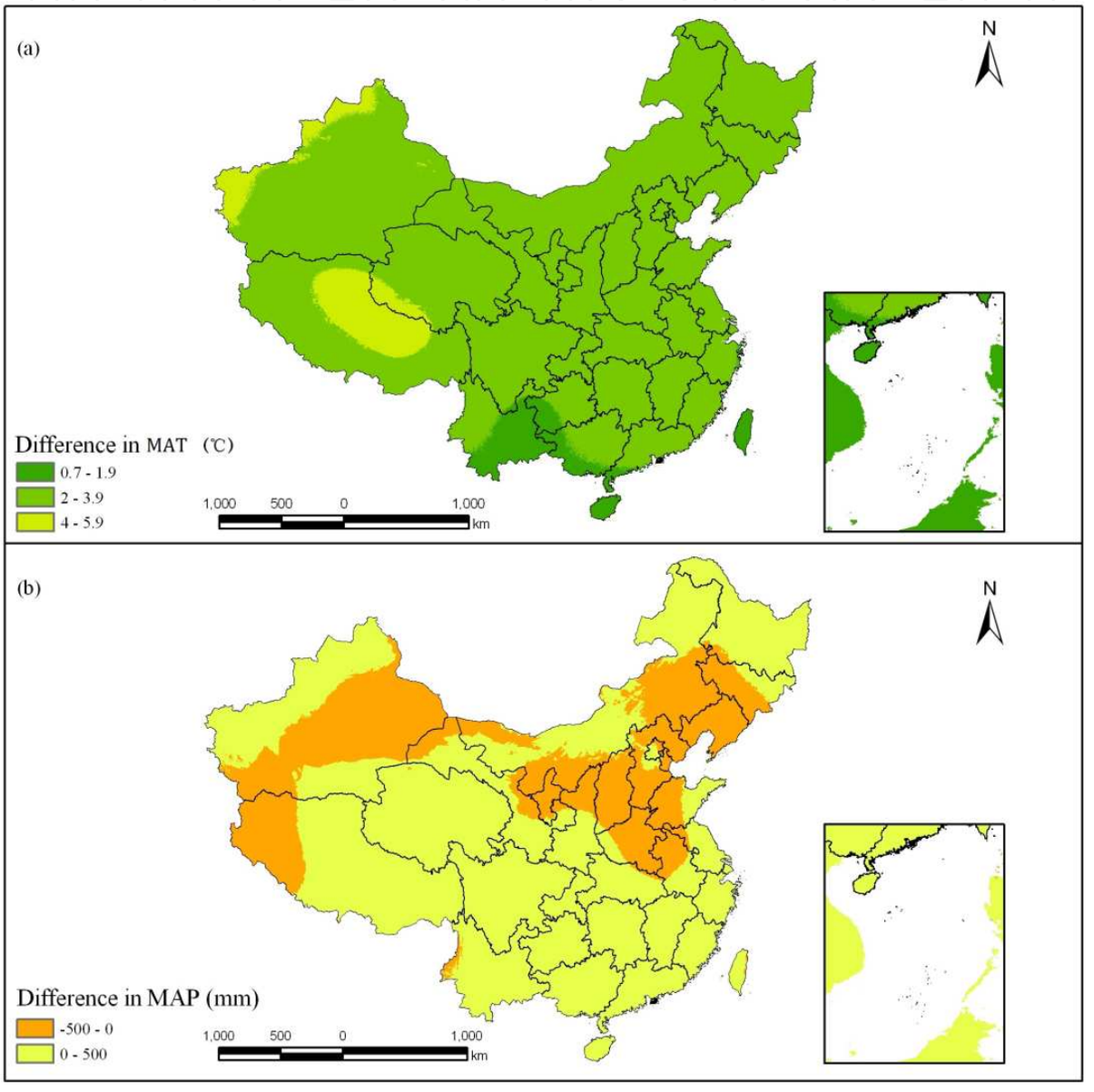

Figure 17. Maps of changes under the future climatic A2a scenario (1950-2000) relative to the average for 1950-2000 for (a) mean annual temperature (MAT) and (b) mean annual precipitation (MAP) in China.

http://dx.doi.org/10.5772/57297

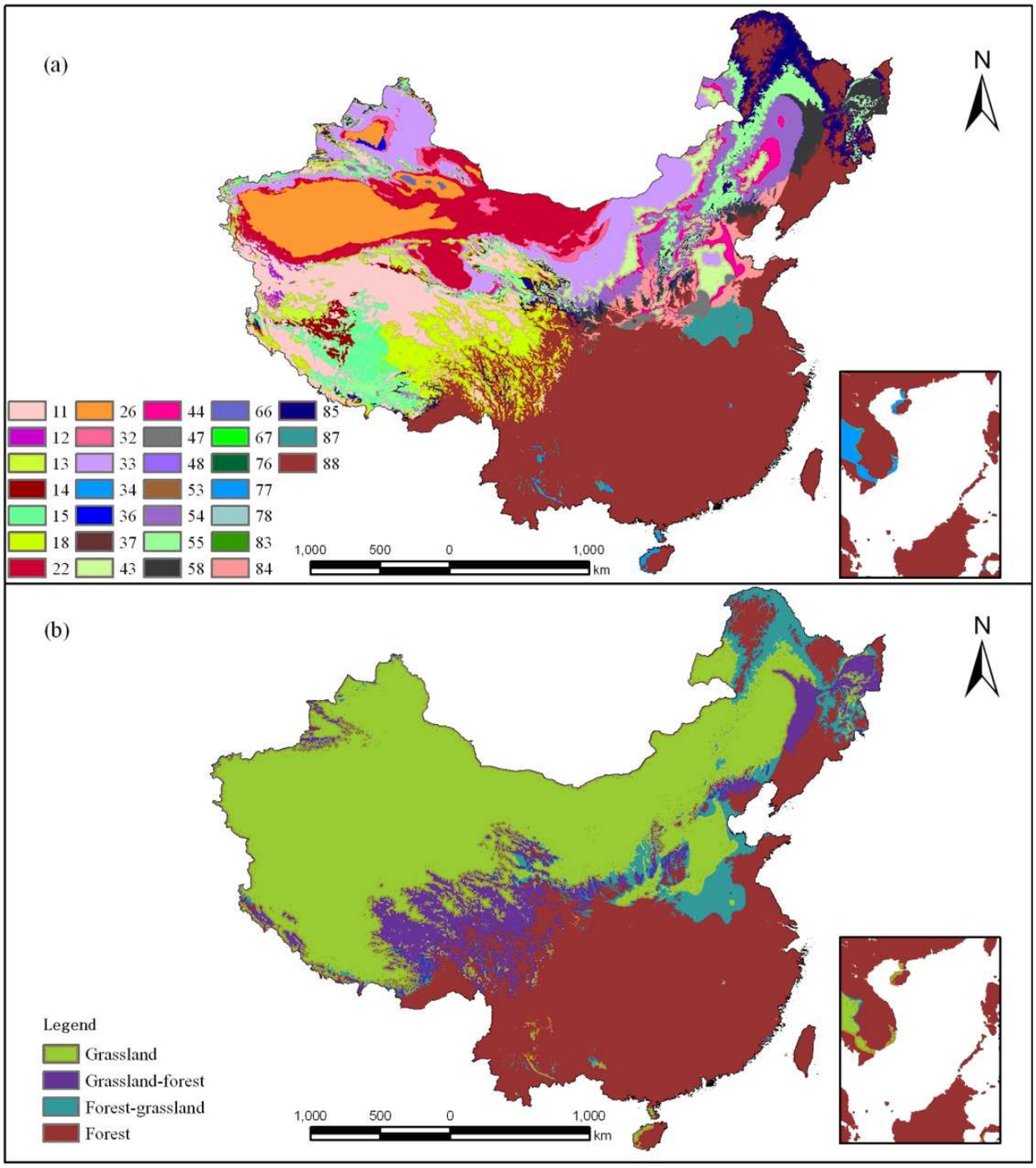

Figure 18. Spatial distribution dynamics of potential biomes in China from the recent past to the future (2001-2050) in the A2a scenario.

Code	China	Inner Mongolia Autonomous Region	Tibet Autonomous Region	Gansu Province	Qinghai Province	Xinjiang Uygur Autonomous Region	Heilongjiang Province
11	83.54	-	39.62	1.29	24.41	18.76	-
12	2.60	-	0.91	0.01	0.03	1.65	-
13	12.95	-	5.66	0.37	1.49	5.44	-
14	8.46	-	5.70	0.32	0.81	1.62	-
15	28.90	-	22.56	0.70	2.31	3.33	-
18	58.02	0.01	23.26	1.67	20.82	2.22	-
22	66.61	18.72	-	11.40	8.41	28.09	-
26	56.94	-	-	0.49	-	56.45	-
32	13.48	3.52	0.30	2.37	0.71	6.57	-
33	62.17	22.95	0.16	4.47	3.98	26.51	-
36	0.81	-	-	-	-	0.81	-
37	0.06	-	-	0.01	-	-	-
43	28.53	12.77	0.07	1.73	0.44	3.35	-
44	18.81	8.33	0.01	0.38	0.48	0.58	0.12
47	4.64	-	-	0.08	-	-	-
53	0.76	-	0.03	0.03	-	0.71	-
54	43.72	18.49	0.55	3.06	1.07	3.34	3.45
55	33.00	12.15	3.86	1.04	2.16	1.59	6.76
58	23.36	0.20	0.72	2.66	0.02	0.07	8.77
66	0.80	-	-	-	-	0.80	-
77	1.25	-	-	-	-	-	-
78	0.09	-	-	-	-	-	-
84	18.26	-	0.03	1.52	-	-	-
85	36.31	10.62	2.95	1.36	2.08	1.32	14.10
87	12.64	-	-	0.13	-	-	-
88	329.27	6.93	14.33	5.50	2.52	0.46	12.02

Note: The symbols are defined in the same way as in Table 8.

Table 11. Projected changes in area(million hectares) of biome conversions from 1950 to 2050

An area of 81.5 million hectares of the Grassland category would be converted to the Forest category and 67.2 million hectares of the Forest category would be converted into the Grassland

http://dx.doi.org/10.5772/57297

category (Figure 18b and Tables 4, 10, 11). There is a clear trend for a decrease in the area of the Grassland category by 11.1 million hectares, whereas areas of the Forest category would increase by 11.3 million hectares (Tables 4, 10 and 11). The relative area of the Forest category would increase by 2.7% over this period (1950-2050), whereas the relative area of the Grassland category would decrease by 2.1% over the same period.

4.4.3.3. Change in TNPP

The Classification Indices-based Model shows NPP either neutral or increasing for most Chinese grid cells during the periods from the recent past through the A2a scenario (Figure 19). At the class level, the largest increases would be in Subtropical-humid evergreen broad-leaved forest (VIE 34), Tropical-per-humid rain forest (VIIF 42), Subtropical per-humid evergreen broad-leaved forest (VIF 41), Subtropical-subhumid sclerophyllous forest (VID 27), and Tropical-humid seasonal rain forest (VIIE 35), as a result of increased MAT and MAP in southern China. The TNPP of Warm temperate-semi-arid warm temperate typical steppe (IVC, 18) in the north-east of the Inner Mongolia Plateau and the Plain of Northern China would increase by 71.69 Tg C year^{-1} because of increased precipitation in these regions. Warmer temperatures would be primarily responsible for increases in NPP in the Tibet Autonomous Region, i.e., the TNPP of Warm temperate-arid warm temperate zonal semi-desert (IVB 11), Cold temperate per-humid taiga forest (IIF 37), and Cold temperate-humid montane meadow (IIE 30) would increase, whereas the TNPP of Frigid per-humid rain tundra, alpine meadow (IF 36) would decrease sharply. The TNPP of Cool temperate-arid temperate zonal semi-desert (IIIB 10) in both the middle of the Xinjiang Uygur Autonomous Region and the northern area of the Inner Mongolia Autonomous Region would show a marked decrease due to decreased precipitation (Table 12).

Biome (super-class group)	Class-ID	China		Inner Mongolia Autonomous Region		Tibet Autonomous Region		Gansu Province		Qinghai Province		Xinjiang Uygur Autonomous Region	
		Recent past	A2a	Recent past	A2a	Recent past	A2a	Recent past	A2a	Recent past	A2a	Recent past	A2a
Tundra and alpine steppe	IA1	0.10	2.44	-	-	-	0.24	-	-	-	-	0.10	0.11
	IB8	37.93	57.01	-	-	9.45	30.04	0.14	0.05	0.90	0.13	22.65	26.78
	IC15	31.53	39.20	-	-	11.32	19.66	0.18	0.12	0.66	0.74	14.28	18.69
	ID22	41.24	46.78	-	-	20.36	27.82	0.21	0.34	0.59	2.04	14.62	16.58
	IE29	91.93	106.91	-	-	55.21	77.19	0.33	2.16	1.00	8.34	24.73	19.23
	IF36	2304.27	887.90	0.25	-	1032.10	321.61	3.49	17.82	45.98	420.81	164.80	76.11
Frigid desert	IIA2	18.12	10.75	-	-	-	3.70	0.38	0.12	10.33	0.70	7.41	6.22
	IIIA3	128.53	57.75	44.26	0.01	-	-	36.31	11.83	9.62	27.20	38.33	18.71
	IVA4	214.23	278.30	38.47	110.28	-	-	12.36	52.25	-	-	163.40	115.77
Semi-desert	IIB9	54.70	110.24	0.04	-	2.30	41.86	6.38	5.88	17.71	17.79	28.28	44.70
	IIIB10	691.68	463.69	313.17	271.30	-	0.01	60.47	22.08	19.65	44.18	266.21	124.96

Biome (super-class group)	Class-ID	China		Inner Mongolia Autonomous Region		Tibet Autonomous Region		Gansu Province		Qinghai Province		Xinjiang Uygur Autonomous Region	
		Recent past	A2a	Recent past	A2a	Recent past	A2a	Recent past	A2a	Recent past	A2a	Recent past	A2a
Steppe	IVB11	188.23	793.74	38.62	318.08	-	-	8.51	71.95	-	0.30	92.40	276.57
	VB12	2.14	267.67	-	-	-	-	0.17	0.08	-	-	-	0.71
	IIC16	40.90	110.53	3.26	-	0.68	66.13	3.37	4.21	7.00	11.72	26.59	28.47
	IIIC17	597.23	483.52	414.72	342.19	-	8.80	35.78	17.42	5.90	22.27	31.95	51.72
	IVC18	519.03	1235.92	2.49	279.73	0.31	4.67	4.37	107.37	-	6.05	-	10.31
	VC19	117.75	509.91	-	-	-	0.62	1.56	19.49	-	-	-	-
	IVD25	841.62	849.66	-	6.07	0.72	16.09	61.37	119.16	-	0.58	-	2.12
Temperate humid grassland	IID23	62.18	187.51	14.37	0.05	4.53	138.15	4.05	4.80	9.43	18.23	29.68	26.27
	IIID24	976.28	594.58	397.16	263.99	9.38	59.84	63.01	25.79	10.86	31.26	15.83	30.75
	IIE30	208.57	323.66	75.29	0.17	55.82	233.95	10.61	8.16	24.67	43.97	40.26	37.40
Warm desert	VA5	0.39	109.54	-	-	-	-	-	0.28	-	-	0.39	109.26
	VIA6	-	0.74	-	-		-		-		-		0.74
Savanna	VIB13	1.47	117.36	-	-	-	-	-	1.32	-	-	-	-
	VIIB14	3.85	7.68	-	-	-	-	-	-	-	-	-	-
	VIC20	31.08	568.06	-	-	-	-	0.02	8.37	-	-	-	-
	VIIC21	30.73	61.80	-	-	-	-	-	-	-	-	-	-
Forest, including Temperate forest, Sub-tropical forest and Tropical forest	VD26	583.92	393.29	-	-	-	0.35	2.50	20.88	-	-	-	-
	VID27	219.17	1299.22	-	-	-	-	-	1.80	-	-	-	-
	VIID28	90.26	189.93	-	-	-	-	-	-	-	-	-	-
	IIIE31	1247.72	1240.25	209.53	322.60	24.87	62.07	104.06	36.77	11.71	36.23	6.52	23.37
	IVE32	1118.61	925.41	-	-	1.64	54.73	48.60	47.17	-	-	-	-
	VE33	2050.76	755.60	-	-	-	4.75	-	0.69	-	-	-	-
	VIE34	1911.89	3859.07	-	-	-	0.20	-	-	-	-	-	-
	VIIE35	622.82	1623.86	-	-	-	-	-	-	-	-	-	-
	IIF37	1502.54	1879.78	388.80	81.96	229.04	611.51	96.39	75.86	95.61	546.35	33.71	49.97
	IIIF38	1827.77	1456.20	34.63	105.08	96.09	177.73	56.28	70.14	0.53	31.00	0.18	8.03
	IVF39	1904.99	1027.94	-	-	119.58	71.14	0.82	2.83	-	-	-	-
	VF40	3402.34	1221.15	-	-	99.21	75.22	-	-	-	-	-	-
	VIF41	5166.77	6509.44	-	-	229.74	231.03	-	-	-	-	-	-
	VIIF42	628.69	2177.01	-	-	54.25	203.87	-	-	-	-	-	-

Note: The class name refers to Fig.7. Explanation

Table 12. Comparison of the total net primary productivity (10^{11} g C) of biomes and classes of 1950-2000(recent past) with those of 2000-2050 under A2a scenario

http://dx.doi.org/10.5772/57297

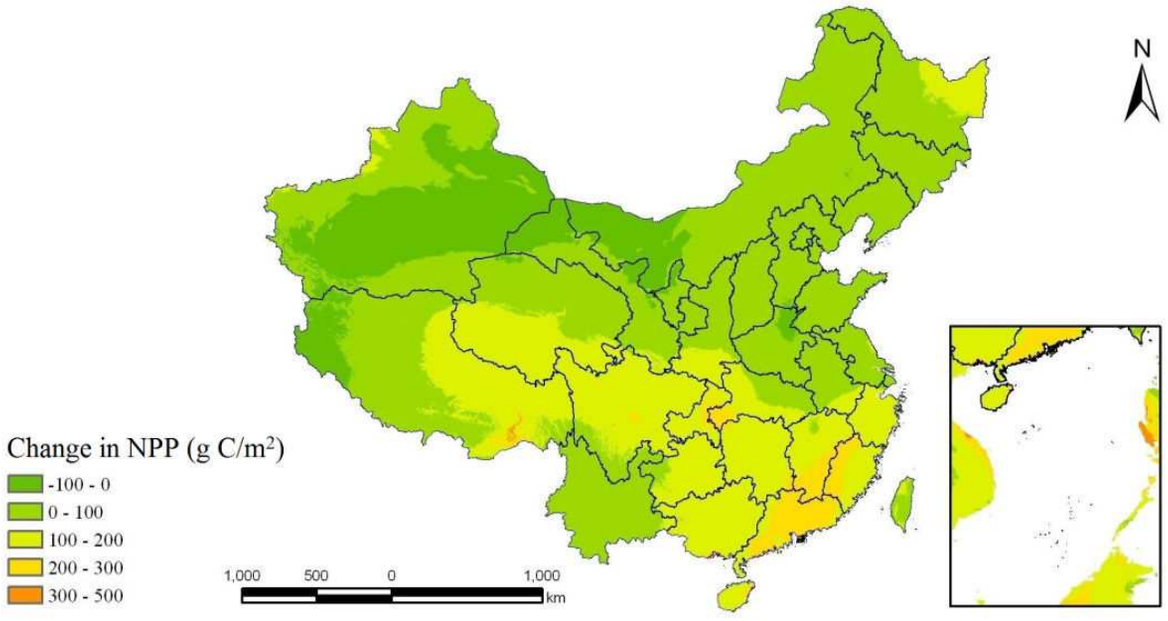

Figure 19. Trend of Changes in net primary productivity (NPP) from the recent past to the future (2001-2050) in the A2a scenario. The changes show the differentiated NPP, and negative values indicate C loss for NPP.

At the grassland biome level, the TNPP of Steppe would show the largest increase, followed by Semi-desert, Savanna and Warm desert. These increases in TNPP are 107.3, 69.9, 68.8 and 11.0 Tg C, respectively. The TNPP of Tundra and alpine steppe would show the largest decrease, followed by Temperate humid grassland and Cold desert. The simulated TNPP of Tundra and alpine steppe would decrease by 136.7 Tg C compared with its size during 1950-2000. The decrease of TNPP for Temperate humid grassland and Cold desert would be 14.1 Tg C and 1.4 Tg C, respectively (Tables 4, 10 and 12).

At the category level, the TNPP of Grassland category would increase by 14.5% to 104.7 Tg C over this period (1950-2050), whereas the TNPP of Forest category would increase by 10.2% to 228.0 Tg C (Tables 4, 10 and 12).

4.4.4. Discussion

4.4.4.1. Grassland carbon budgets

The Classification Indices-based Model projects China's TNPP at 3.28 Pg C (Table 10) under the future climatic A2a scenario and is close to the projections of 3.33 and 3.34 Pg C by the Vegetation Interaction Model (AVIM) [91] and the CEVSA (Carbon Exchange between Vegetation, Soil, and Atmosphere) model [92], both derived by using long-term annual average data (1980-2005). The results could potentially favor China's position in supporting its effort to reduce global warming gas as outlined in the Kyoto Protocol. The model outputs suggest that the potential TNPP of grasslands in China is 0.83 Pg C in the A2a scenario (Table 10).

Climate change is expected to affect the TNPP of grassland. Understanding climate and NPP feedback cycles in grasslands requires knowledge of the changes in spatial patterns on the NPP of grasslands. The dynamic change characteristics of potential biomes (Table 12 and Figure 18) highlights the risk that China's grassland faces with a climate that is 'already hot, dry and variable' [85] under global warming. The Classification Indices-based Model estimated an increase of 104.71Tg C in TNPP for potential grasslands from recent past to the future A2a scenario. The increase in TNPP for grasslands at northern latitudes was mainly driven by increased temperature and, in lower latitudes, by changes in precipitation (Figure 17 and Figure 19). The increase in TNPP for grasslands will bring an increase of 375.5 Tg of annual sequestration of CO_2 and 276.4 Tg of annual contribution to the atmospheric O_2 cycle respectively (1.63g of CO_2 are absorbed and 1.2 g of O_2 are released to generate 1g of dry matter according to photosynthesis stoichiometry) [89].

4.4.4.2. 'Safe' livestock carrying capacity

The goal of sustainable livestock husbandry is to balance the consumption of forage by livestock with the annual production of the grassland, so that future grassland production is not diminished. The concept of a 'safe' livestock carrying capacity was developed to estimate the capacity of the grassland resource to sustainably carry livestock (and other herbivores) in the long term (>30 years) [83]. Predictions of NPP give a good estimate of the annual production of the grasslands, and therefore NPP can be used to balance the food demands of different kinds of livestock, allowing a calculation of the maximum carrying capacity of livestock that can be supported on the grassland. This maximum carrying capacity of the grassland should be used to develop appropriate policies of grazing control to preserve sustainable production on the grassland [16]. The implication of climate change projections for 'safe' livestock carrying capacity remains an open question. Global warming causes changes in temperature and precipitation patterns, resulting in fluctuations in the NPP of grasslands. Several researchers have predicted that increases in temperature will cause a shift in the ratio of C_4 to C_3 grasses, with C_4 increasing [17, 93]. This may decrease carrying capacity, since C_4 grasses are generally considered to be of lower nutritive value to grazing animals than C_3 species [94]. Moreover, increasing temperature and declining precipitation are also considered to decrease dietary crude protein, protein availability, and digestible organic matter [93]. In situations where climates become warmer and drier, grazing livestock are likely to encounter a protein-limited diet. The future declines in forage quality would also produce greater methane production from ruminant livestock [93]. Thus, it is important to assess climate change projections in terms of their implications for future 'safe' livestock carrying capacity and the risk of resource degradation [83]. However, the questions of what the 'safe' livestock carrying capacity is and of how best to integrate a wide range of factors, such as grassland classes, climatic variability and animal nutrition, are unresolved. So further research and development is needed to identify the regional trends for the 'safe' livestock carrying capacity to maintain sustainable resource condition and reduce the risk of resource degradation. This important task remains a challenge for all grassland scientists and practitioners.

http://dx.doi.org/10.5772/57297

Acknowledgements

The research was funded by the National Natural Science Foundation of China (No. 31172250) and the project of the Humanities and Social Sciences Planning Fund of the Chinese Ministry of Education (No. 10YJAZH047). This chapter is dedicated to Wanquan Lin, the father of Huilong Lin, who left this earth on July 3, 2013. He was a source of constant encouragement, wise counsel, and a remarkable example of hard work, integrity and a loving father.

Author details

Huilong Lin*

Address all correspondence to: linhuilong@lzu.edu.cn

State Key Laboratory of Grassland Agro-Ecosystems, College of Pastoral Agriculture Science and Technology, Lanzhou University, Lanzhou City, China

References

[1] Hui DF, Jackson RB. Geographical and interannual variability in biomass partitioning in grassland ecosystems: a synthesis of field data. New Phytologist 2006; 169 85-93.

[2] Scurlock JM, Hall D. The global carbon sink: a grassland perspective. Global Change Biology 1998; 4 229-233.

[3] Scurlock LMO, John K, Olson RJ. Estimating net primary productivity from grassland biomass dynamics measurements. Global Change Biology 2002; 8 736-753.

[4] Del Grosso S, Parton W, Stohlgren T, et al. Global potential net primary production predicted from vegetation class, precipitation, and temperature. Ecology 2008; 89 2117-2126.

[5] Holdridge LR. Determination of world plant formations from simple climatic data. Science 1947; 105 367-368.

[6] Lieth H. Modelling the primary productivity of the world. Nature and Resources 1972; 8 (2) 5-10.

[7] Uchijima Z. An agroclimatic method of estimating net primary productivity of natural vegetation. JARQ 1988; 21 244-250.

[8] Uchijima Z, Seino H. Agroclimatic evaluation of net primary productivity of natural vegetation. I. Chikugo model for evaluating net primary productivity. Journal of Agricultural Meterology 1985; 40 343-352(in Japanese with English summary).

[9] Zaks DPM, Ramankutty N, Barford CC, et al. From Miami to Madison: Investigating the relationship between climate and terrestrial net primary production. Global Biogeochemical Cycles 2007; 21 GB3004, DOI: 10. 1029/2006GB002705.

[10] Zhou GS, Zhang XS. A natural vegetation NPP model. Acta Phytoecologica Sinica 1995; 19(3) 193-200 (In Chinese with English abstract).

[11] Zhou GS, Wang YH, Jiang YL, et al. Estimating biomass and net primary production from forest inventory data: a case study of China's Larix forests. Forest Ecology and Management 2002; 169 149-157.

[12] Zhu ZH. A model for estimating net primary productivity of natural vegetation. Chinese Science Bulletin 1993; 38(22) 1913-1917.

[13] Melillo JM, Mcguire AD, Kicklighter DW, et al. Global climate change and terrestrial net primary production. Nature 1993; 363 234-240.

[14] Adams B, White A, Lenton TM. An analysis of some diverse approaches to modelling terrestrial net primary productivity. Ecological Modelling 2004; 177 353-391.

[15] Schuur EAG. Productivity and global climate revisited: the sensitivity of tropical forest growth to precipitation. Ecology 2003; 84 1165-1170.

[16] Zhang GG, Kang YM, Han GD, et al. Effect of climate change over the past half century on the distribution, extent and NPP of ecosystems of Inner Mongolia. Global Change Biology 2011; 17 377-389.

[17] Ren JZ, Hu ZZ, Zhao J, et al. A Grassland classification system and its application in China. The Rangeland Journal 2008; 30 199-209.

[18] Lobo A, Rebollar JL. Model-based discriminant analysis of Iberian potential vegetation and bio-climatic indices. Physics and Chemistry of the Earth 2010; 35 52-56.

[19] Zhou GS, Wang YH. Global change and climate-vegetation classification, Chinese Science Bulletin 2000; 45 577-584.

[20] Liang TG, Feng QS, Cao JJ, et al. Changes in global potential vegetation distributions from 1911 to 2000 as simulated by the Comprehensive Sequential Classification System approach. Chinese Science Bulletin 2012; 57 1298-1310.

[21] Kaplan JO, Bigelow NH, Prentice IC, et al. Climate change and arctic ecosystems II: Modelling , paleodata-model comparisons, and future projections. Journal of geophysical research 2003; 108 8171.

[22] Lin HL. A New Model of Grassland Net Primary Productivity (NPP) Based on the Integrated Orderly Classification System of Grassland. In: Chen YX, Deng HP, Zhang DG, et al (eds). The Sixth International Conference on Fuzzy Systems and Knowl-

edge Discovery. Tianjing, IEEE Computer Society Conference Publishing Services 2009; (1) 52-56. DOI: 10. 1109/FSKD. 2009. 705

[23] Liang TG, Feng QS, Huang XD, et al. Advance in the Study of Integrated Orderly Classification System of Grassland. Acta prataculture sinica 2011; 20 (3) 79-82(in Chinese with English abstract).

[24] Lin HL, Zhao J, Liang TG, et al. A Classification indices-based model for net primary productivity (NPP) and potential productivity of vegetation in China. International Journal of Biomathematics 2012; 5(3) 1-23. DOI: 10. 1142/S1793524512600091

[25] Lin HL, Zhang YJ. Evaluation of six methods to predict grassland net primary productivity along an altitudinal gradient in the Alxa Rangeland, Western Inner Mongolia, China. Grassland Science 2013; 59 100-110. DOI: 10. 1111/grs. 12019.

[26] Zhang L, Wylie B, Loveland T, et al. Evaluation and comparison of gross primary production estimates for the Northern Great Plains grasslands. Remote Sensing of Environment 2007; 106 173-189.

[27] Lin HL, Feng QS, Liang TG, et al. Modelling global-scale potential grassland changes in spatio-temporal patterns to global climate change. International Journal of Sustainable Development & World Ecology 2013; 20(10) 83-96.

[28] Lin HL, Wang XL, Zhang YJ, et al. Spatiotemporal dynamics on the distribution, extent and NPP of potential grassland in response to climate changes in China. The Rangeland Journal 2013;35(4) 409-425. DOI: 10. 107/RJ12024.

[29] Nash JE, Sutcliffe JV. River flow forecasting through conceptual models. Part 1. A discussion of principles. Journal of Hydrology 1970; 10 282-290.

[30] Lin HL, Zhuang QM, Fu H. Habitat Niche-fitness and Radix Yield Prediction Models for Angelica sinensis Cultivated in the Alpine Area of the Southeastern Region of Gansu Province, China. Plant Production Science 2008; 11(1) 42-58.

[31] Whittaker RH. A criticism of the plant association and climatic climax concepts. Northwest Science 1951; 25 17-31.

[32] Ni J. Net primary productivity in forests of China: scaling-up of national inventory data and comparison with model predictions. Forest Ecology Management 2003; 176 485-495.

[33] Ni J. Forage yield-based carbon storage in grasslands of China. Climatic Change 2004a; 67 237-246.

[34] Ni J. Estimating net primary productivity of grasslands from field biomass measurements in temperate northern China. Plant Ecology 2004b; 174 217-234.

[35] Kang L, Han XG, Zhang ZB, et al. Grassland ecosystems in China: review of current knowledge and research advancement. Philosophical Transactions of the Royal Society B: Biological Sciences 2007; 362 997-1008.

[36] Akiyama T, Kawamura K. Grassland degradation in China: Methods of monitoring, management and restoration. Grassland Science 2007; 53 1-17.

[37] Jiang Y, Kang MY, Liu S, et al. A study on the vegetation in the east side of Helan Mountain. Plant Ecology 2000; 149 119-130.

[38] Lieth H, Box E. Evapotranspiration and primary productivity. In: Memorial Model (Ed Thornthwaite W). Publications in Climatology. New Jersey: Intech; 1972. p37-46.

[39] Zhou GS, Zhang XS. Study on Chinese climate-vegetation relationship. Acta Phytoecologica Sinica 1996; 20 (2) 113-119(In Chinese with English abstract).

[40] Long SP, Garcia Moya E, Imbamba SK, et al. Primary productivity of natural grass ecosystems of the tropics: a reapprisal. Plant and Soil 1989; 115 155-166.

[41] Ren JZ. Research methods of grassland science. China Agricultural Press, Beijing, China: Intech; 1998. (In Chinese).

[42] Ohta S, Uchijima Z, Oshima. Probable effects of CO_2-induced climatic changes on net primary productivity of terrestrial vegetation in East Asia. Ecological Research 1993; 8 199-213.

[43] Fisher JB, Whittaker RJ, Malhi Y. ET come home: potential evapotranspiration in geographical ecology. Global Ecology and Biogeography 2011; 20 1-18.

[44] Fang JY, Song YC, Liu HY, et al. Vegetation-Climate Relationship and Its Application in the Division of Vegetation Zone in China. Acta Botanica Sinica 2002; 44(9) 1105-1122.

[45] Wang P, Sun R, Hua J, et al. Measurements and simulation of forest leaf area index and net primary productivity in Northern China. Journal of Environmental Management 2007; 85 607-615.

[46] Nadler IA, Wein RW. Spatial interpolation of climate normals: test of a new method in the Canadian boreal forest, Agricultural and Forest Meteorology 1998; 92(4) 211-225.

[47] Zhao J, Li F, Fu HY, et al. A DEM-based partition adjustment for the interpolation of annual cumulative temperature in China. In Geoinformatics 2007: Geospatial Information Science (Proceedings of the SPIE) 2007; 6753 6753.

[48] Sun R, Zhu QJ. Distribution and Seasonal Change of Net Primary Productivity in China from April, 1992 to March, 1993. Acta Geographica Sinica 2000; 55 36-45(in Chinese with English abstract).

[49] Feng QS, Liang TG, Huang XD, et al. Characteristics of global potential natural vegetation distribution from 1911 to 2000 based on comprehensive sequential classfication system approach. Grassland Science 2013; 59 87-99. DOI: 10. 1111/grs. 12016

[50] Piao SL, Fang JY, He JS, et al. Spatial distribution of grassland biomass in China. Acta Phytoecologica Sinica 2004; 28(4) 491-498(in Chinese with English abstract).

[51] Ni J. Carbon storage in grassland of China. Journal of Arid Environments 2002; 50 205-218.

[52] Yu DY, Shao HB, Shi PJ, et al. How does the conversion of land cover to urban use affect net primary productivity? A case study in Shenzhen city, China. Agricultural and Forest Meteorology 2009; 149(11) 2054-2060.

[53] Fang JY, Piao SL, Tang ZY, et al. Interannual variability in net primary productivity and precipitation. Science 2001; 293 1723.

[54] Piao SL, Fang JY, Ciais PP, et al. The carbon balance of terrestrial ecosystems in China. Nature 2009; 458 1009-1013.

[55] Haberl H. Human appropriation of net primary production as an environmental indicator: implications for sustainable development. Ambio 1997; 26(3) 143-146.

[56] Haberl H, Krausmann F, Erb KH, et al. Human appropriation of net primary production. Science 2002; 296 1968-1969.

[57] Krausmann F. Land use and industrial modernization: an empirical analysis of human influence on the functioning of ecosystems in Austria 1830-1995. Land Use Policy 2001; 18 17-26.

[58] Kohlheb N, Krausmann F. Land use change, biomass production and HANPP: The case of Hungary 1961-2005. Ecological Economics 2009; 69(2) 292-300.

[59] Haberl H, Plutzar CK. Erb H, et al. Human appropriation of net primary production as determinant of avifauna diversity in Austria. Agriculture, Ecosystems & Environment 2005; 110 119-131.

[60] Haberl H, Gaube V, Delgado RD, et al. Towards an integrated model of socioeconomic biodiversity drivers, pressures and impacts: A feasibility study based on three European long-term socio-ecological research platforms. Ecological Economics 2009; 68(6) 1797-1812.

[61] OmannI, Stocker A, Jäger J. Climate change as a threat to biodiversity: An application of the DPSIR approach. Ecological Economics 2009; 69(1) 24-31. DOI: 10. 1016/j. ecolecon. 01. 003.

[62] Haberl H, Schulz NB, Plutzar C, et al. Human appropriation of net primary production and species diversity in agricultural landscapes. Agricultural Ecosystem Environment 2004; 102(2) 213-218.

[63] Vitousek PM, Ehrlich PR, Ehrlich AH, et al. Human appropriation of the products of photosynthesis. BioScience 1986; 36 363-373.

[64] Anderson JM. The effects of climate change on decomposition processes in grassland and coniferous forests. Ecological Application 1991; 1(3) 326-347.

[65] White R, Murray S, Rohweder M. Pilot analysis of global ecosystems (PAGE): grassland ecosystems. Washington, DC: World Resources Institute: Intech; 2000.

[66] Liang TG, Feng QS, Yu H, et al. Dynamics of natural vegetation on the Tibetan Plateau from past to future using a comprehensive and sequential classification system and remote sensing data. Grassland Science 2012; 58 208-220.

[67] Hutchinson MF. Anusplin Version 4. 3. Centre for Resource and Environmental Studies. Canberra (Australia): The Australian National University 2004.

[68] Hijmans RJ, Cameron SE, Parra JL, et al. Very high resolution interpolated climate surfaces for global land areas. International Journal of Climatology 2005; 25 1965-1978.

[69] New M, Hulme M, Jones P. Representing twentieth-century space-time climate variability. Part I: Development of a 1961-90 mean monthly terrestrial climatology. Journal of Climate 1999; 12 829-856.

[70] New M, Lister D, Hulme M, et al. A high-resolution data set of surface climate over global land areas. Climate Research 2002; 21 1-25.

[71] Jarvis CH, Stuart N. A comparison among strategies for interpolating maximum and minimum daily air temperatures. Part II: the interaction between the number of guiding variables and the type of interpolation method. Journal of Applied Meteorology and Climatology 2001; 40 1075-1084.

[72] Potter CS, Randerson JT, Field CB, et al. Terrestrial ecosystem production: a process model based on global satellite and surface data. Global Biogeochemical 1993; 70(4) 811-841.

[73] Zhang J, Ishii J, Fujikura K. A biogeochemistry approach on the bivalves: REE distribution of white clam in Off Hatsushima cold seepage. Chinese Science Bulletin 1999; 44(supp.) 258-260.

[74] Alexandrov GA, Oikawa T, Esser G. Estimating terrestrial NPP: what the data say and how they may be interpreted? Ecological Modelling 1999; 117(2-3) 361-369.

[75] Feng YM, Lu Q, Wu B, et al. Landuse dynamics of alpine-cold decertified area in the Qinhai-Tibetan Plateau in the last 30 years: a case study in Guinan County, Qinghai Province, China. International Journal of Sustainable Development & World Ecology 2011; 18(4) 357-365.

[76] Ge QS, Dai JH, Zheng JY, et al. Advances in first bloom dates and increased occurrences of yearly second blooms in eastern China since the 1960s: further phonological evidence of climate warming. Ecological Research 2011; 26 713-723.

[77] Piao SL, Fang JY, Chen AP. Seasonal Dynamics of Terrestrial Net Primary Production in Response to Climate Changes in China. Acta Botanica Sinica 2003; 45(3) 269-275.

[78] Twine TE, Kucharik CJ. Climate impacts on net primary productivity trends in natural and managed ecosystems of the central and eastern United States. Agricultural and Forest Meteorology 2009; 149(12) 2143-2161.

[79] Zheng YR, Xie ZX, Robert C, et al. Did climate drive ecosystem change and induce desertification in Otindag sandy land, China over the past 40 years? Journal of Arid Environments 2006; 64 523-541.

[80] Harle KJ, Howden SM, Hunt LP, et al. The potential impact of climate change on the Australian wool industry by 2030. Agricultural Systems 2007; 93 61-89.

[81] Henry BK, McKeon GM, Syktus JI, et al. Climate variability, climate change and land degradation. In: Sivakumar MVK and Ndiang'ui N editors. Climate and Land Degradation. Berlin: Springer-Verlag 2007; 205-221.

[82] Howden SM, Crimp SJ, Stokes CJ. Climate change and its effect on Australian livestock systems. Australian Journal of Experiment Agriculture 2008; 48(7) 780-788.

[83] McKeon GM, Stone GS, Syktus JI, et al. Climate change impacts on northern Australian rangeland livestock carrying capacity: a review of issues. The Rangeland Journal 2009; 31 1-29.

[84] Friedlingstein P, Delire C, Muller JF, et al. The climate induced variation of the continental biosphere: a model simulation of the Last Glacial Maximum. Geophysical Research Letters 1992; 19 897-900.

[85] IPCC. Climate change. 2007: Synthesis Report. Contribution of Working Groups I, II and III to the Fourth Assessment Report of the Intergovernmental Panel on Climate Change. Geneva, Switzerland: Intech; 2007.

[86] Evangelista PH, Kumar S, Stohlgren TJ, et al. Assessing forest vulnerability and the potential distribution of pine beetles under current and future climate scenarios in the Interior West of the US. Forest Ecology and Management 2011; 262 307-316.

[87] Yang HJ, Wu MY, Liu WX, et al. Community structure and composition in response to climate change in a temperate steppe. Global Change Biology 2011; 17 452-465.

[88] Liu WX, Zhang Z, Wan SQ. Predominant role of water in regulating soil and microbial respiration and their responses to climate change in a semiarid grassland. Global Change Biology 2009; 15(1) 184-195.

[89] Dong XB, Yang WK, Ulgiati S, et al. The impact of human activities on natural capital and ecosystem services of natural pastures in North Xinjiang, China. Ecological Modelling 2012; 225 28-39.

[90] Naustdalslid J. Climate change-the challenge of translating scientific knowledge into action. International Journal of Sustainable Development & World Ecology 2011; 18(3) 243-252.

[91] He Y, Dong WJ, Ji JJ, et al. The net primary production simulation of terrestrial ecosystems in China by AVIM. Advance in Earth Science 2005; 20 345-349 (in Chinese with English abstract).

[92] Gao ZQ, liu JY. Simulation study of China's net primary production. Chinese Science Bulletin 2008; 53(3) 434-443.

[93] Craine JM, Elmore AJ, Olson KC, et al. Climate change and cattle nutritional stress. Global Change Biology 2010; 16 2901-2911.

[94] Ehleringer JR, Cerling TE, Dearing MD. Atmospheric CO_2 as a global change driver influencing plant-animal interactions. Integrated and Comparative Physiology 2002; 42 424-430.